

# Exploring a new machine learning based probabilistic model for high-resolution indoor radon mapping, using the German indoor radon survey data

Eric Petermann<sup>1</sup>, Peter Bossew<sup>1,2</sup>, Joachim Kemski<sup>3</sup>, Valeria Gruber<sup>4</sup>, Nils Suhr<sup>1</sup>, Bernd Hoffmann<sup>1</sup>

1 – Section Radon and NORM, Federal Office for Radiation Protection (BfS), Berlin, Germany

2 – retired

3 – Sachverständigenbüro Dr. Kemski, Bonn, Germany

4 - Department for Radon and Radioecology, Austrian Agency for Health and Food Safety (AGES), Linz, Austria

Corresponding author: Eric Petermann, [epetermann@bfs.de](mailto:epetermann@bfs.de), Köpenicker Allee 120-130, 10318 Berlin, Germany

The authors declare they have no conflicts of interest related to this work to disclose.

Keywords: indoor air, Germany, quantile regression forest, public exposure, residential buildings

Abstract:

Background: Radon is a carcinogenic, radioactive gas that can accumulate indoors. Therefore, accurate knowledge of indoor radon concentration is crucial for assessing radon-related health effects or identifying radon-prone areas.

Objectives: Indoor radon concentration at the national scale is usually estimated on the basis of extensive measurement campaigns. However, characteristics of the sample often differ from the characteristics of the population due to the large number of relevant factors that control the indoor radon concentration such as the availability of geogenic radon or floor level. Furthermore, the sample size usually does not allow estimation with high spatial resolution. We propose a model-based approach that allows a more realistic estimation of indoor radon distribution with a higher spatial resolution than a purely data-based approach.

Methods: A two-stage modelling approach was applied: 1) a quantile regression forest using environmental and building data as predictors was applied to estimate the probability distribution function of indoor radon for each floor level of each residential building in Germany; (2) a probabilistic Monte Carlo sampling technique enabled the combination and population weighting of floor-level predictions. In this way, the uncertainty of the individual predictions is effectively propagated into the estimate of variability at the aggregated level.

Results: The results show an approximate lognormal distribution with an arithmetic mean of 63 Bq/m<sup>3</sup>, a geometric mean of 41 Bq/m<sup>3</sup> and a 95 %ile of 180 Bq/m<sup>3</sup>. The exceedance probability for 100 Bq/m<sup>3</sup> and 300 Bq/m<sup>3</sup> are 12.5 % (10.5 million people) and 2.2 % (1.9 million people), respectively. In large cities, individual indoor radon concentration is generally lower than in rural areas, which is due to the different distribution of the population on floor levels.

Discussion: The advantages of our approach are 1) an accurate estimation of indoor radon concentration even if the survey was not fully representative with respect to the main controlling factors, and 2) an estimate of the indoor radon distribution with a much higher spatial resolution than basic descriptive statistics.

## 1. Introduction

The radioactive noble gas radon is a human carcinogen.<sup>1,2</sup> A causal association between radon exposure and the risk of developing lung cancer has been established<sup>3</sup>, a possible association with other diseases is currently under scientific discussion.<sup>4-6</sup> The adverse health effects of radon are known for uranium miners<sup>7</sup> and have also been shown to be associated with indoor radon exposure at home<sup>3,8</sup>. Radon is one of the most important causes of lung cancer after smoking. Further, smoking and radon reinforce each other in their harmful effects on human health. Gaskin<sup>9</sup> estimated the number of annual deaths due to indoor radon exposure at 266,000 worldwide (for 66 countries; 74 % of world's population) making radon responsible for approximately 3 % of the approximately 10 million cancer deaths per year worldwide reported by the International Association of Cancer Research in 2020.<sup>10</sup>

In most cases, the main source of indoor radon is the soil and rock under the house, where radon (Rn-222) is generated by decay of radium (Ra-226), a progeny of uranium (U-238). Radon concentration is measured by its radioactive activity in becquerel (decay processes per second) per m<sup>3</sup> (unit: Bq/m<sup>3</sup>). As a component of natural radioactivity, radon is present in all soils and rocks, but with distinct spatial variation regarding its concentration (e.g., see European Atlas of Natural Radiation<sup>11</sup>). Radon enters houses mainly via advective transport, driven by temperature- and wind-induced pressure difference, via small cracks and fissures in the buildings' foundation<sup>12,13</sup>. Secondary sources of indoor radon are building materials containing elevated radionuclide levels<sup>14,15</sup>, water supply (especially when water is drawn directly from private wells)<sup>16-18</sup>, natural gas<sup>16,19</sup> and, in some specific cases, outdoor air<sup>20,21</sup>. The accumulation of radon indoors depends on the exchange with (usually) low radon outdoor air and is controlled by the air tightness of the building and the ventilation rate. In most cases, indoor radon concentration is higher on the lower floors than on the upper floors because the lower floors are closer to the ground and thus closer to the main source of radon.<sup>14,22</sup>

The estimation of regional or national indoor radon concentration is usually achieved by large-scale measurement campaigns. These measurement campaigns have to be representative so that the sample reflects the relevant characteristics of the population (e.g., availability of geogenic radon, distribution of people on different floors, building types) and thus provides an unbiased estimate. Therefore, sampling design should ensure representativeness, e.g. by taking random samples from some type of national registry (e.g. postal addresses, buildings, telephone numbers)<sup>23-25</sup>. In these cases, sampling density is proportional to the population density and the sample should reflect the spatial distribution of dwellings and/or people across the country. Subsequently, the measured data are usually aggregated for the spatial scale of interest, and the desired statistical characteristics can be derived. However, even with a population-weighted sampling design, bias may occur e.g., because participation is voluntary and people who know that they are exposed to a higher hazard (e.g. people living on lower floors) might be aware of this fact and may be more motivated to participate. Therefore, even with population-weighted sampling, the characteristics of the sample must be compared with the characteristics of the population also with regard to building-related factors. In general, although being a key factor governing indoor radon concentration<sup>14,26-28</sup>, the distribution of the population

across floors is often not considered<sup>24,29,30</sup> – probably due to the lack of appropriate data. However, some commendable exceptions, where the distribution of the population across floors has been explicitly considered, exist such as in Vienneau et al. for Switzerland<sup>31</sup>.

It is important to note, that the purpose of many studies which focus on mapping indoor radon is not necessarily to estimate national indoor radon exposure, but rather to delineate hazard areas. For the latter, a common approach is to define a reference house such as in studies for Austria<sup>32</sup>, Germany<sup>33</sup>, South Korea<sup>34</sup>, Switzerland<sup>35</sup> or in the European Atlas of Natural Radiation<sup>11</sup>. The results of these studies, although reporting statistics of indoor radon values, cannot easily be used for estimating national indoor radon concentration because predictions were made for a defined situation (e.g., ground floor) and thus do not reflect the variability of housing conditions within the population.

To overcome the limitations described above, predictive models are widely applied as a complementary tool for concentration estimation by utilizing available information on the relevant variables that govern indoor radon. The advantages of applying a model-based approach are three-fold: 1) it allows correction of a potential sampling bias (lack of sample representativeness), 2) estimation at unmeasured locations is possible and 3) it allows a higher spatial resolution if sufficiently highly resolved predictor data are available. Application of a predictive model requires that spatially exhaustive information on relevant factors is available (e.g., soil radon map, national building registry). If this information is known not only globally (e.g. at the national scale in this case), but also on a higher resolved scale (e.g. at state or district level) a predictive model can also be used to estimate at a higher spatial resolution. This approach is very useful because a robust estimation of indoor radon concentration at high spatial resolution based solely on measured data would require an enormous number of measurements, which would drastically increase the financial and logistical effort.

Machine learning models have been increasingly used to model indoor radon in recent years<sup>31,36-41</sup>. These studies consistently report on machine learning models' superior performance compared to previous approaches. However, predictive models – also those based on machine learning – are only able to explain a certain amount of the observed variability due to the absence of relevant information (e.g., the information on air tightness of an individual building, resident behaviour with respect to ventilation frequency and intensity) or that predictor data does not sufficiently reflect local characteristics (e.g., outcrop of a (unmapped) small-scale geological unit). As a consequence, predictions of indoor radon at the individual level, i.e. building, dwelling, floor level or room, usually have a large uncertainty which is manifested by a low predictive performance for point estimates. The amount of prediction uncertainty also affects the estimation of the radon distribution of a population since the distribution of predictions (i.e., expected values) have the tendency to be considerably smoothed in comparison to the observed distribution. For example, Vienneau et al.<sup>31</sup> estimated indoor radon for Switzerland using a machine learning based model under consideration of many relevant predictors. In this study the expected indoor radon concentration for each resident in Switzerland was estimated. This approach will - although being accurate for estimating the national mean - underestimate the true variability of indoor radon concentration in the population because it does not explicitly account for prediction uncertainty. Therefore, the circumstance that many people will be exposed to radon concentrations which are substantially deviating from the expected value (i.e., the conditional mean) is not considered and thus the estimation of quantities such as the exceedance probability of certain threshold values (e.g., 300 Bq/m<sup>3</sup>) are doomed to fail. Consequently, to derive realistic estimates of certain quantiles or exceedance probabilities, propagation of prediction uncertainty is required.

The overall goal of our study is to characterize the distribution of indoor radon concentration in Germany at different administrative levels (country, federal state, district, municipality). We have chosen model-based approach to represent variability of environmental and building-related

characteristics within the population and to enable the characterization (incl. exceedance probabilities) of indoor radon concentration at a high spatial resolution.

## 2. Data & Methods

### 2.1. Survey description

A population-weighted national indoor radon survey was carried out in Germany from 2019-2021. In total, 7,479 households participated and each household was equipped with two passive solid-state nuclear track detectors. Participants were asked to conduct measurements in two different occupied rooms. There were no specific behavioural instructions (e.g. on ventilation behaviour), as the measurement campaign was intended to reflect typical conditions over the course of a year. A population-representative sample was aimed by determining a target number of participants per district (“Landkreise und kreisfreie Städte”;  $n=401$  in 2019) which was proportional to the population size of the respective district i.e., more measurements took place in districts with more inhabitants. The actual number of measurements differed from the target number in some cases, resulting in an over- or under-representation of certain districts (see Figure S1).

A number of relevant building- and household-related characteristics were documented using a questionnaire. The target measurement duration of 365 days (with a tolerance of  $\pm 10\%$ ) was achieved by 14,053 measurements. These data (Fig. 1) were used for further analysis in this study. Details on the survey design can be found in S1.

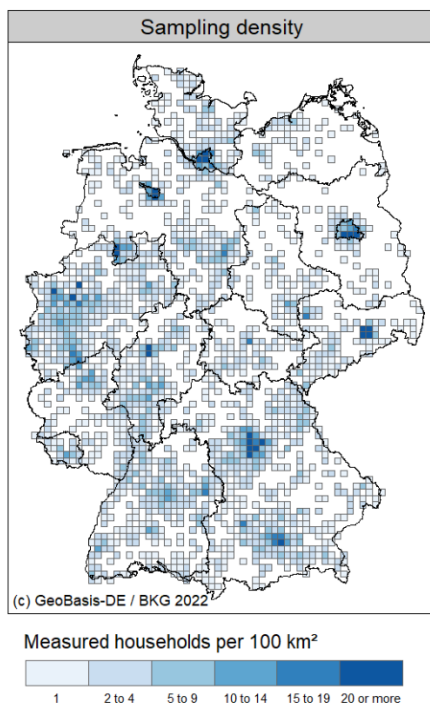


Figure 1: Sampling density of households participating in the new national indoor radon survey of Germany. Sampling density was proportional to the population density at the district level („Landkreise und kreisfreie Städte“). Consequently, more measurements were taken in urban areas than in rural areas. Generally, two measurements were made in each household ( $n=7,479$ ).

### 2.2. Predictor data

Predictor data were selected because of their expected potential impact on indoor radon. Numerous studies have shown a clear dependence of indoor radon on geogenic radon availability (e.g.,<sup>14,33,42-48</sup>). Furthermore, many studies (e.g.,<sup>16,28,38,49</sup>) have also proven an association between indoor radon concentration and climate/weather conditions (temperature, precipitation, soil moisture) which resulted in temporal variability of indoor radon on hourly to seasonal time-scales. Also, wind speed has been identified as an influential parameter governing indoor radon by affecting the pressure gradient indoor/outdoor<sup>49,50</sup>. Slope has also been found to have some explanatory power for indoor

radon modelling<sup>34,38</sup>. Different studies identified tectonic faults as the cause of locally increased geogenic radon<sup>51,52</sup>. Regarding dwelling characteristics, floor level<sup>14,26-28,53</sup> and age of building<sup>14,18,43,45,53,54</sup> have consistently been reported to be main governing factors of indoor radon concentration. Some studies have also identified an influence of building type on indoor radon<sup>14,16,43,54</sup>. The expected association of the used predictors and indoor radon are briefly summarized in the following:

- age of building might be a proxy for air tightness of the foundation as well as building design (including building material),
- climate-related predictors (outdoor temperature, annual precipitation) could be a proxy for building design, ventilation intensity, living habits
- the slope inclination affects the contact area with the ground; a higher contact area could enhance radon entry rates
- soil gas permeability and soil moisture affect soil radon generation and transport in the ground
- wind exposure might be a proxy for typical pressure gradients between building and atmosphere which govern advective radon influx from soil to building
- building type and number of living units affect building design and could be a proxy for living habits and ventilation intensity
- geological faults represent areas where radon transport can be enhanced locally, i.e. areas with high fault density may be susceptible to increased geogenic radon supply

#### 2.2.1. Environmental data

Environmental predictor data comprise mapped quantities of soil, climate, terrain and geology. Soil related quantities are the soil radon concentration, soil gas permeability and soil moisture. Soil radon concentration and soil gas permeability reflect the conditions in 1 m depth and are based on measurements collected by the Federal Office for Radiation Protection (BfS). Maps were produced at 500 m resolution using a random forest model. Details can be found in S2. Climate data of soil moisture<sup>55</sup>, annual precipitation<sup>56</sup> and average outdoor temperature<sup>57</sup> were taken from the German Weather Service (DWD). Terrain characteristics were calculated based on a digital elevation model at a 25 m resolution<sup>58</sup>. The wind exposure index reflects the relative terrain position and is a dimensionless index with higher values indicating stronger exposure to wind (for details on calculation see S2). Tectonic fault density (expressed as fault line length in m per ha) is based on the faults mapped in the geological map of Germany at a scale of 1:250,000<sup>59</sup>. Radon concentration in outdoor air (1.5 m height) were produced using a random forest model at 500 m resolution. Details on generating and/or processing of environmental data can be found in S2. Summary statistics on assigned environmental data to indoor radon survey data is given in Supplemental Excel file; table S1.

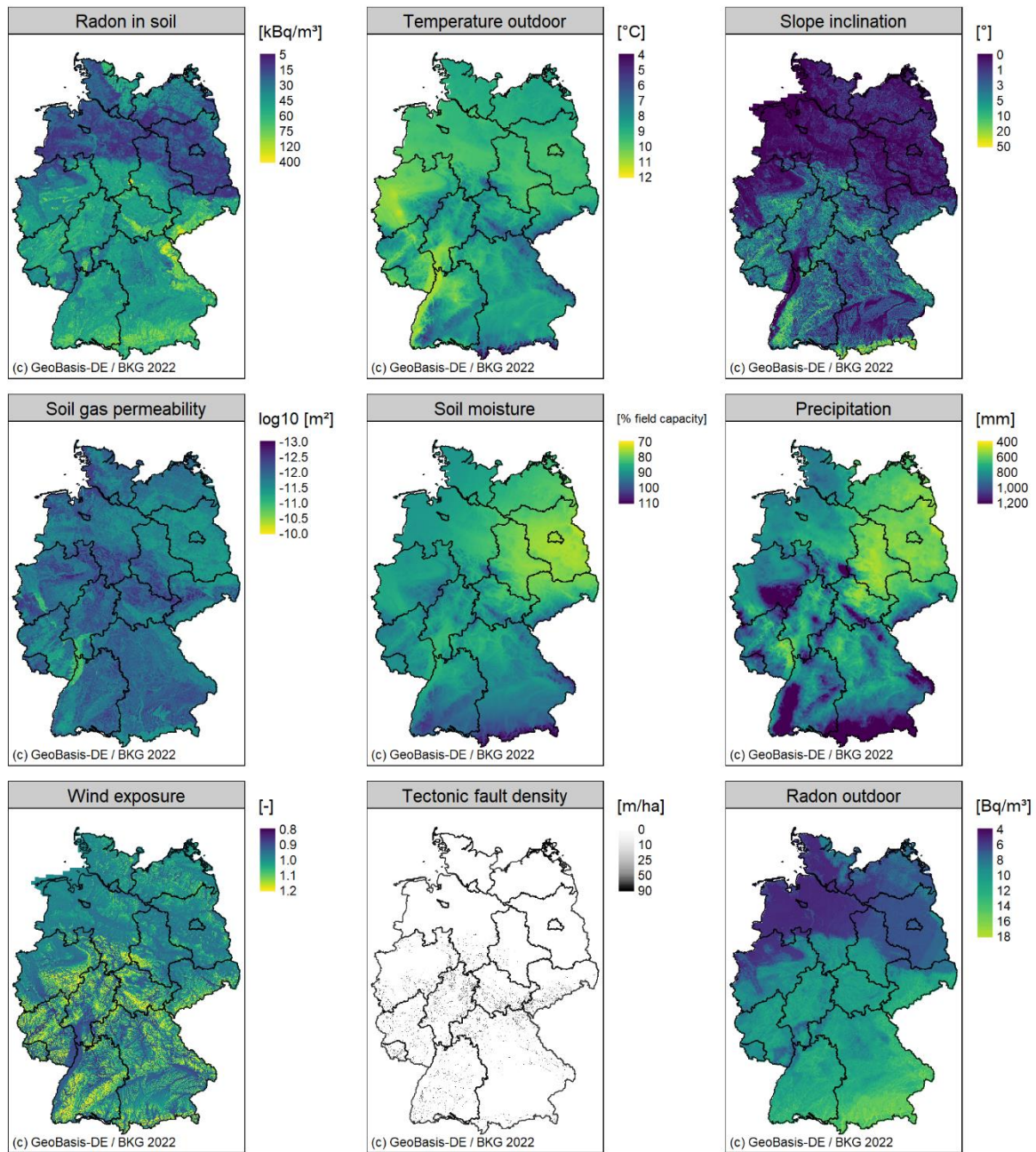


Figure 2: Environmental data providing information on soil: radon in soil and soil gas permeability (source: Federal Office for Radiation Protection, BfS) ; climate: outdoor temperature , soil moisture and precipitation (source: German Weather Service, DWD); terrain: slope and wind exposition (derived from digital elevation model; source: Federal Agency for Cartography and Geodesy, BKG); geology: tectonic fault density (source: Federal Institute for Geosciences and Natural Resources, BGR). Data were spatially joined with indoor radon measurements and used as predictors in the quantile regression forest model. Outdoor radon was used for improving the fit of a distributional function fitted to quantile predictions.

### 2.2.2. Building-related data

Building-related data were derived from a georeferenced data set published by the Federal Agency for Geodesy and Cartography.<sup>60</sup> This data set refers to the year 2021 and comprises all buildings in Germany ( $n \approx 21.9$  million). Each building is characterized by a point coordinate. For further analysis, only residential buildings (i.e., buildings with at least 1 inhabitant) were considered ( $n \approx 21.3$  million). Relevant data which were available for each address are:

- number of households

- number of inhabitants
- number of floor levels
- age of building (for information on classification see S3)
- building type (for information on classification see S3)

Due to some discrepancies in class definitions between survey-related and building-related datasets, class definitions regarding age of building and building type were harmonized (see S3 for details) to allow predictions for the entire residential building stock. Summary statistics on assigned building data to indoor radon survey data is given in Supplemental Excel file; table S2.

### 2.2.3. Floor-level distribution of the population

The number of people per floor level was estimated using data on the number of floor levels and the number of inhabitants per building. We assumed an equal distribution of people across all floor levels from the ground floor to the uppermost floor level of the building.

Basements, which usually have the highest radon levels within a building, are widespread in Germany ( $\approx 90\%$  of the measured houses have a full or partial cellar). In a considerable number (30%) of the participating households, measurements were carried out in basements (mostly used as workrooms). However, no external data was available on the occurrence and the use of basements. Therefore, assumptions about the use of basements were necessary in order to take them sufficiently into account in the estimation of radon concentration.

Considering that basement occupation depends on the building type, we assumed that basements are more frequently used in single- and two-family houses as well as in townhouses compared to multi-family houses or apartment blocks. Therefore, we parameterized basement occupation as follows (see also S4 for illustration):

- (1) For building types “single- and two-family house”, “townhouses/row houses and semi-detached houses”: 30% of the occupation of each upper floor level (see S4)
- (2) For building type “multi-family houses”, “(high-rise) apartment blocks: 5% of the occupation of each upper floor level (see S4)

## 2.3. Modelling approach

The modelling approach (see Figure 3) was based on a multistage procedure:

- 1) Model building: The data from the national survey and relevant predictor data (fig. 2) were used to train a regression model that is able to predict conditional quantiles on the dwelling-scale.
- 2) Prediction: The model was applied to make a prediction of conditional quantiles for each floor level of each residential building in Germany. Based on the quantile predictions and assuming lognormality, a probability density function (PDF) was fitted for each floor level of each residential building.
- 3) Monte Carlo sampling: probabilistic samples were drawn from each PDF. The sample size was proportional to the number of inhabitants. Thus, different PDFs were combined and population-weighted.
- 4) Aggregation: The data of generated probabilistic samples in 3) were aggregated on the administrative level of interest (national, federal states, districts, municipality) and the desired statistical characteristics such as the arithmetic mean or the probability to exceed  $300 \text{ Bq/m}^3$  were calculated.

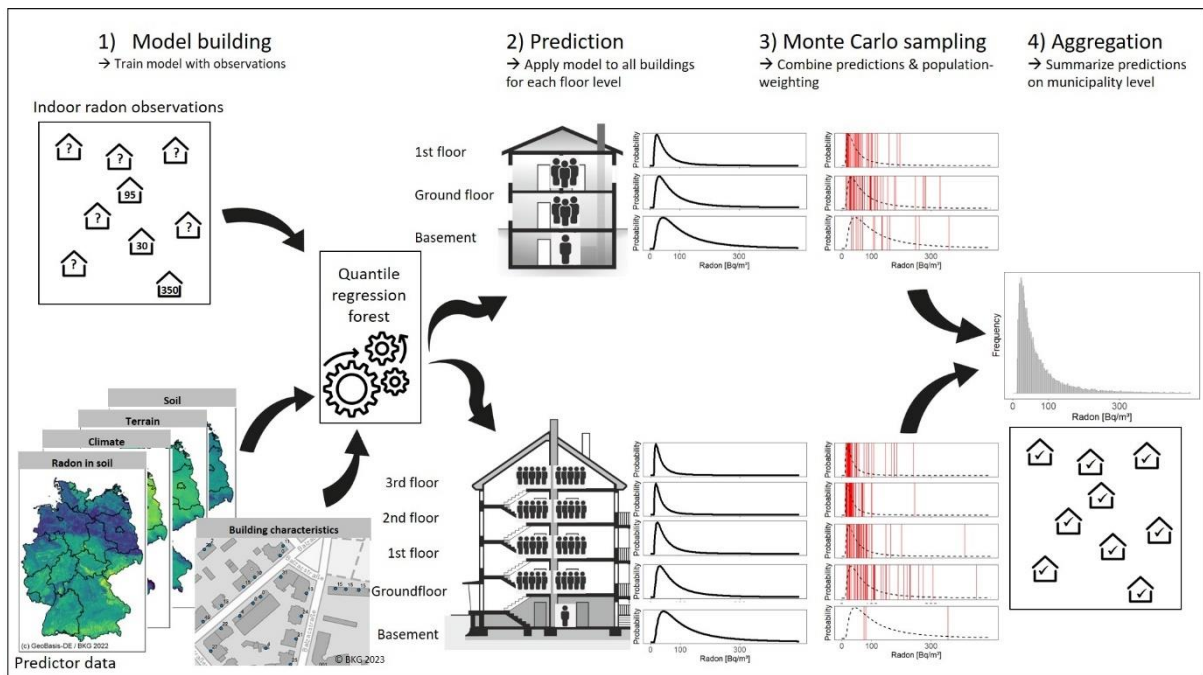


Figure 3: Schematic figure of the applied modelling approach: 1) Model building: training of the quantile regression forest model using indoor radon observations ( $n=14,053$ ) and twelve environmental and building-related predictors; 2) Prediction of probability distribution functions (PDFs) for each floor of each residential building; 3) Monte Carlo sampling: probabilistic sampling from PDFs with sample size proportional to population distribution; 4) aggregation of probabilistic samples on the municipality scale.

### 2.3.1. Quantile regression forest

Quantile regression forest (QRF) is a machine learning algorithm. It is a variation of the well-established Random Forest algorithm. Random Forest was introduced by Breiman<sup>61</sup> and represents an ensemble of regression or classification trees. Data of the target variable is partitioned into smaller, statistically more homogeneous subsets by finding optimal values in the predictor parameter space to split on. Individual trees are aggregated into an ensemble, i.e. the forest. This step drastically reduces the variance in the prediction and leads to more stable predictions. In this study, the implementation in the R package *partykit*<sup>62</sup> was used. In contrast to the classical implementation by Breiman, the function *cforest* in *partykit* builds conditional inference trees<sup>63</sup> using statistical test procedures both for predictor selection at the splits and for the definition of stopping criteria.<sup>64</sup>

Quantile regression forests were introduced by Meinshausen<sup>65</sup>, who showed that Random Forest can be used to predict not only the conditional mean, but also the entire conditional distribution. The ability of QRF to predict the full conditional distribution is based on the fact that it stores the values of all observations in each leaf (i.e., node) of the tree and not just the mean as in the standard Random Forest. Knowing the full conditional distribution allows for straightforward estimation of prediction intervals. By estimating the distribution from an ensemble of realisations, QRF follows the same approach as conditional simulation in classical geostatistics.

### 2.3.2. Model building and prediction

Model building generally follows the approach described by Petermann et al.<sup>66</sup>. In short, 15 candidate predictors were spatially joined with locations of indoor radon observations. The loss function was the RMSE (root mean squared error). Since the target variable “indoor radon concentration” has a skewed (near log-normal) distribution and the fact that it was not transformed before model training, high observations were implicitly given more weight, i.e. high observations had a greater leverage on model fit.

Predictors were selected by forward feature selection (R package *CAST*<sup>67</sup>) via a spatial 10-fold cross-validation approach. The size of spatial blocks (squares in our case) was set to 40 km (R package *blockCV*<sup>68</sup>). The motivation for predictor selection is to find only those predictors which are informative and thus contribute to improving the predictive performance of the model. The final set of selected predictors consisted of eight environmental predictors (radon in soil, outdoor temperature, slope, soil permeability, soil moisture, precipitation, wind exposure, tectonic faults; see Fig. 2) and four building-related predictors (floor level, age of the building, building type and number of households). The hyperparameter *mtry* (number of predictors randomly selected and evaluated at each split) was tuned and an optimal value of 4 was found. Then, the final model with selected predictors and *mtry* = 4 was fitted with 500 regression trees (*ntree*) using all available indoor radon observations.

The QRF model was used to make predictions of nine percentiles (10<sup>th</sup>, 25<sup>th</sup>, 50<sup>th</sup>, 75<sup>th</sup>, 80<sup>th</sup>, 85<sup>th</sup>, 90<sup>th</sup>, 95<sup>th</sup>, 98<sup>th</sup>) for each floor level of each residential building in Germany.

The R scripts used for model building and prediction described in 2.3 can be found at [https://github.com/EricPetermann/scripts\\_for\\_IRC\\_prediction\\_Germany](https://github.com/EricPetermann/scripts_for_IRC_prediction_Germany). We created a browser-based web application (<https://model.radonmap.info>) for conducting predictions at the dwelling-scale for user defined locations and building characteristics.

### 2.3.3. Post-processing of model predictions

#### *Distribution fitting*

A distribution function (three-parameter log-normal) was fitted (R package *rriskDistributions*<sup>69</sup>; function *get.lnorm.par*) using data of the predicted quantiles to estimate a probability density function (PDF) for each prediction. The three-parameter log-normal distribution function is very similar to an ordinary log-normal distribution but has a location shift to account for the local background of the quantity of interest. The reason for using a three-parameter lognormal distribution was to avoid indoor radon predictions being lower than the local outdoor radon estimate, which would be implausible from a physical point of view.

To achieve this goal, the local estimate of the outdoor radon concentration (see Fig. 2; S2) was assigned to the predictions by a spatial join. To derive the distribution parameters, the outdoor radon value was subtracted from the predicted indoor radon quantiles, then an ordinary log-normal function was fitted, and finally the outdoor radon value was added after probabilistic sampling. During the fitting process, the higher percentiles were weighted more heavily to optimise the fit in this range. As a result, for each floor level of each residential building, three parameters were determined to describe the probability distribution function (PDF): *meanlog*, *sdlog* and the *offset* (outdoor radon).

#### *Monte Carlo sampling*

Monte Carlo sampling was conducted using the estimated PDF estimated for each floor level (see 2.3.3) (R package *stats*<sup>70</sup>; function *rlnorm*). Random samples are drawn from each PDF for propagation of prediction uncertainty as well as for combining and weighting individual predictions. The sample size was set to be proportional to the population size, i.e. the expected number of inhabitants per floor level was used to weight the individual floor-level based predictions. The sample size was determined by multiplying the expected number of inhabitants per floor level with a factor of 10 and rounded afterwards to guarantee a meaningful representation of all floor levels. This was done because the sample size must be a positive integer and the expected number of inhabitants in many basements is <1. More than 800 million Monte Carlo samples were computed for Germany – a factor of 10 higher than the actual population size (see Fig S4).

### Aggregation of results

A key identifier (“AGS” value) was assigned to each random sample for efficient post-processing. This key allows unequivocal attribution of a random sample to a municipality (“Gemeinde”), district (“Landkreise und kreisfreie Städte”) and federal state (“Bundesland”). Samples were grouped according to the key identifier and desired statistical parameters were calculated: arithmetic mean, arithmetic standard deviation, geometric mean, geometric standard deviation, 50 %ile, 90 %ile, 95 %ile, 99%ile, exceedance probabilities of 100 Bq/m<sup>3</sup>, 300 Bq/m<sup>3</sup>, 600 Bq/m<sup>3</sup> and 1000 Bq/m<sup>3</sup>, respectively. The final set of random samples was split across several csv files due to memory constraints (total size of ~ 22 GB). Therefore, aggregate statistics were calculated utilizing the R packages *arrow*<sup>71</sup> and *dplyr*<sup>72</sup> which allow querying and processing the data without the need of reading data into local memory.

### Computational aspects

The prediction was done for a large data set comprising 21.3 million residential buildings which have on average 2.9 floors. In addition, a prediction was also conducted for the basement. Thus, quantile predictions for ~83 million objects were realized. This setting required to work chunk-wise, i.e. working only on a small subset of the data at once for optimizing computational speed and stability for reading, geoprocessing, predicting, distribution fitting, Monte Carlo sampling and writing of data. The optimal (i.e. fastest overall progress) setting for the chunk size in our case was to process 5000 buildings simultaneously, which resulted in ~4400 chunks. The chunk-wise computation allowed working in parallel and distribute computation across several cores. The entire workflow of the predictive task took approximately 3000 CPU h. The R scripts used for data processing described in 2.3.3 can be found at [https://github.com/EricPetermann/scripts\\_for\\_IRC\\_prediction\\_Germany](https://github.com/EricPetermann/scripts_for_IRC_prediction_Germany).

## 3. Results

### 3.1. Survey results

The descriptive statistics of the survey results show for Germany an arithmetic mean of 78 Bq/m<sup>3</sup> (standard deviation: 126 Bq/m<sup>3</sup>), a geometric mean of 49 Bq/m<sup>3</sup> (geometric standard deviation: 2.32), a 50 %ile of 44 Bq/m<sup>3</sup>, a 90 %ile of 151 Bq/m<sup>3</sup> and a 95 %ile of 241 Bq/m<sup>3</sup>. The exceedance frequencies of the 100 Bq/m<sup>3</sup>, 300 Bq/m<sup>3</sup>, 600 Bq/m<sup>3</sup>, and 1000 Bq/m<sup>3</sup> thresholds were 18 %, 3.5 %, 0.65 %, and 0.35 % of the individual measurements, respectively. Although the spatial distribution of the samples was roughly proportional to the population distribution, a deviation from the population characteristics was observed as a result of sampling bias.

#### 3.1.1. Representativeness regarding floor level

Figure 4 presents the floor distribution of the population in Germany based on the BKG data<sup>60</sup> compared to the distribution of samples in the indoor radon survey. BKG data<sup>60</sup> lack information on basement and souterrain occupancy. Nevertheless, it can be seen that > 30 % of the population live on the second floor or higher, whereas 35 % of the population live on ground floor based on BKG data (Figure 4 upper panel). In contrast, the floor level distribution in the sampled data (Figure 4 lower panel) deviates from the population characteristics as follows: < 10 % of samples are from second floor or higher, > 45 % are from the ground floor. These numbers clearly highlight the tendency of disproportionate high numbers of samples to be from lower floor levels. 15 % of the total samples are from basement floors, also indicating a significant overrepresentation of this floor.

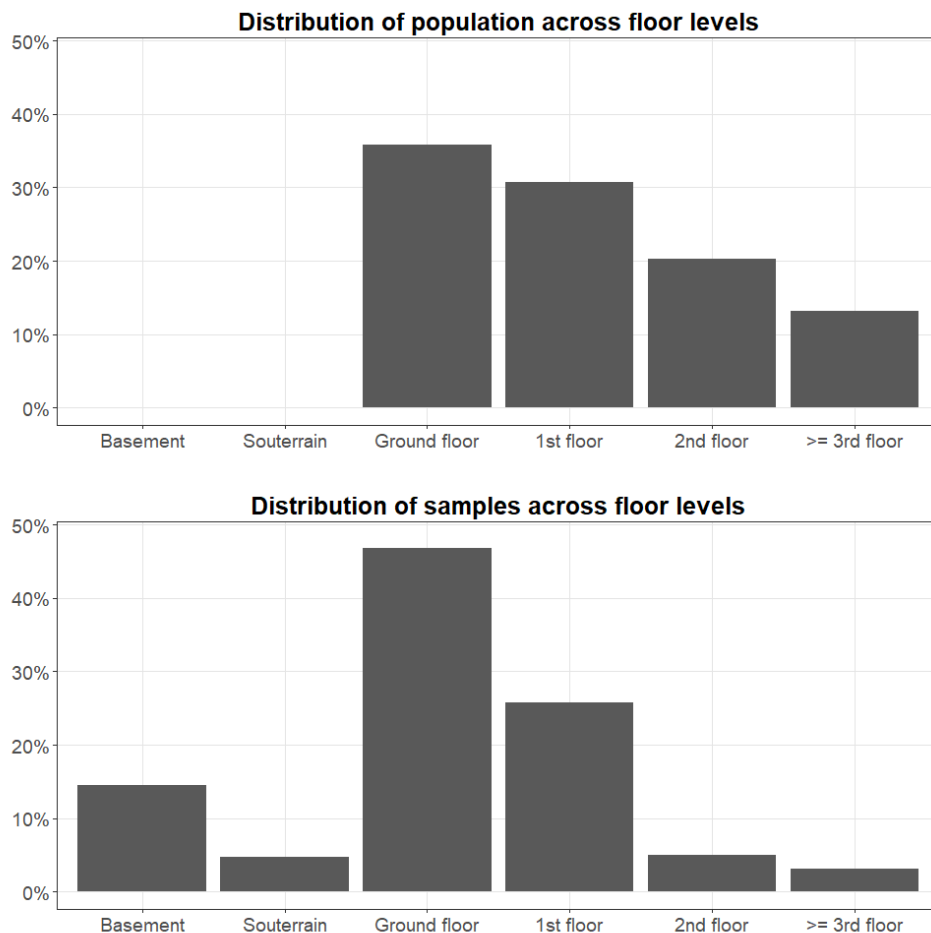


Figure 4: Comparison of sample and population characteristics with respect to floor level distribution. Distribution of population across floor levels (upper plot) is based on residential building stock data (no basement information available;  $n=21.9$  million); distribution of samples across floor levels (lower plot) is based on data provided by participants via questionnaire for each measurement in the national indoor radon survey ( $n=14,053$ ). Data is available in Supplemental Excel file; table S3.

### 3.1.2. Representativeness regarding radon in soil

Another important factor in evaluating the representativeness of the indoor measurements is their distribution with respect to the geogenic radon source. Thus, the distribution of the population with respect to the radon concentration in soil was compared with the distribution of the samples with respect to the radon concentration in soil. For this purpose, the data of population distribution in Germany and sample locations in the indoor radon survey were each spatially linked with the map of radon concentration in soil (see Fig. 2). The resulting distribution is shown as a probability plot in Figure 5. If the sample locations in the survey were fully representative of spatial distribution of the German population with respect to radon concentration in soil, the two curves would be congruent. Indeed, the population and sample distributions are very similar, at least for percentiles 1 to ~ 75. However, for percentiles above 75, both distributions diverge significantly, clearly indicating over-

sampling of areas with high radon risk. The latter could be a result of partially voluntary participation in the survey as described in S1.

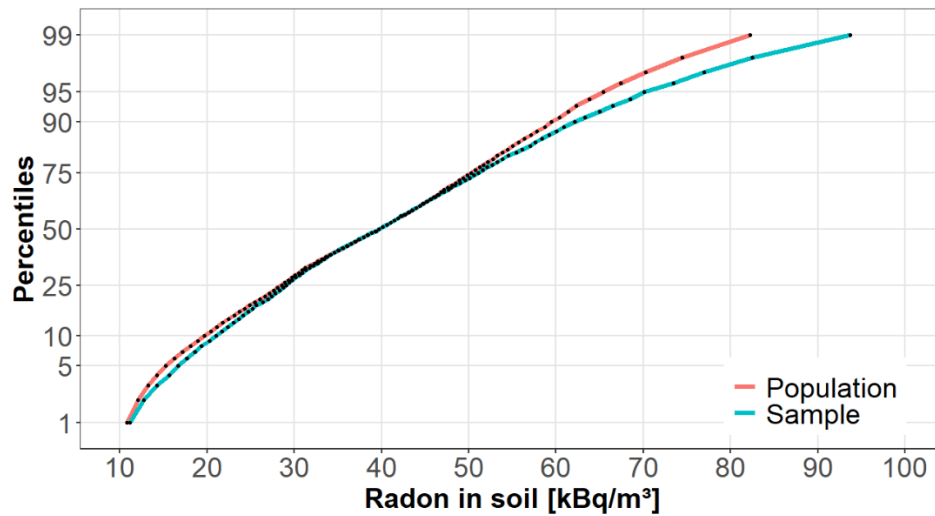


Figure 5: Comparison of sample and population characteristics with respect to radon concentration in soil (see Fig. 2). Values for “Sample” are based on the location of individual measurements in the indoor radon survey ( $n=14,053$ ) and values for “Population” ( $n=83$  million) are based on population distribution in Germany. Data is available in Supplemental Excel file; table S4.

As a result of the data presented in 3.1.1 and 3.1.2 the descriptive statistics of the survey are likely to overestimate the (unknown) true concentration. This is mainly due to 1) an over-sampling of rooms located in more exposed basements and an under-sampling of rooms located in less exposed higher floors, and 2) an over-representation of buildings in areas with higher radon concentration in soil.

## 3.2. Quantile regression forest model

### 3.2.1. Predictor importance

The Quantile regression forest (QRF) model for predicting indoor radon concentration includes twelve predictors which were selected as described in 2.3.2. The importance of the individual predictors in the model was estimated by a permutation-based approach (R package *vip*<sup>73</sup>). The two top predictors are floor level and radon concentration in soil followed by age of building, outdoor temperature and slope. A considerable importance has also been found for soil gas permeability, soil moisture, precipitation, number of living units, wind exposure and building type. The importance of the predictor tectonic faults is negligible in our case. Overall, environmental and building-related predictors are roughly equally important. Information on the effect of individual predictor levels can be derived from the partial dependence plots (see S5).

The predictive model is available as an interactive web application at <https://model.radonmap.info>.

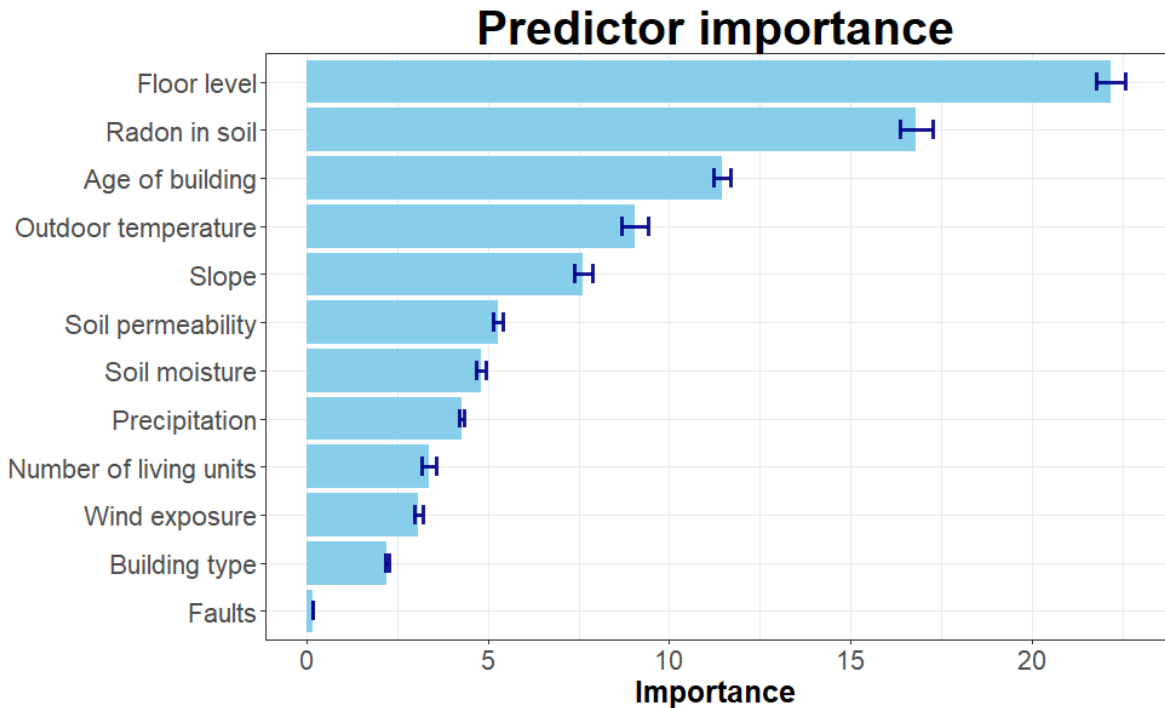


Figure 6: Ranking of predictors by importance for indoor radon prediction with the quantile regression forest model. The importance was measured by calculating the increase of the model's prediction error after permutation (i.e., randomly shuffling values) of the predictor of interest. Data is available in Supplemental Excel file; table S5.

### 3.2.2. Predictive performance

The performance of the predictive model - tested by a 10-fold spatial cross-validation – was analysed with respect to the conditional mean, conditional quantiles and prediction intervals. Predictive accuracy for the conditional mean was sub-optimal, as evidenced by a RMSE of 110.5 and a  $r^2$  (coefficient of determination) of 0.24. Similarly to previous studies<sup>35,66,74</sup>, an underestimation of high values and overestimation of low values was observed, i.e. a general smoothing tendency of the predictions (Figure 7). In Figure 7, observed refers to measured data and predictions refer to modelled values for those locations for which measured data were available.

Performance assessment is likely to provide rather conservative (i.e., overly pessimistic) results due to the spatial blocking approach for data splitting prior to cross-validation, i.e. metrics might actually be better (see Wadoux et al.<sup>75</sup> for discussion).

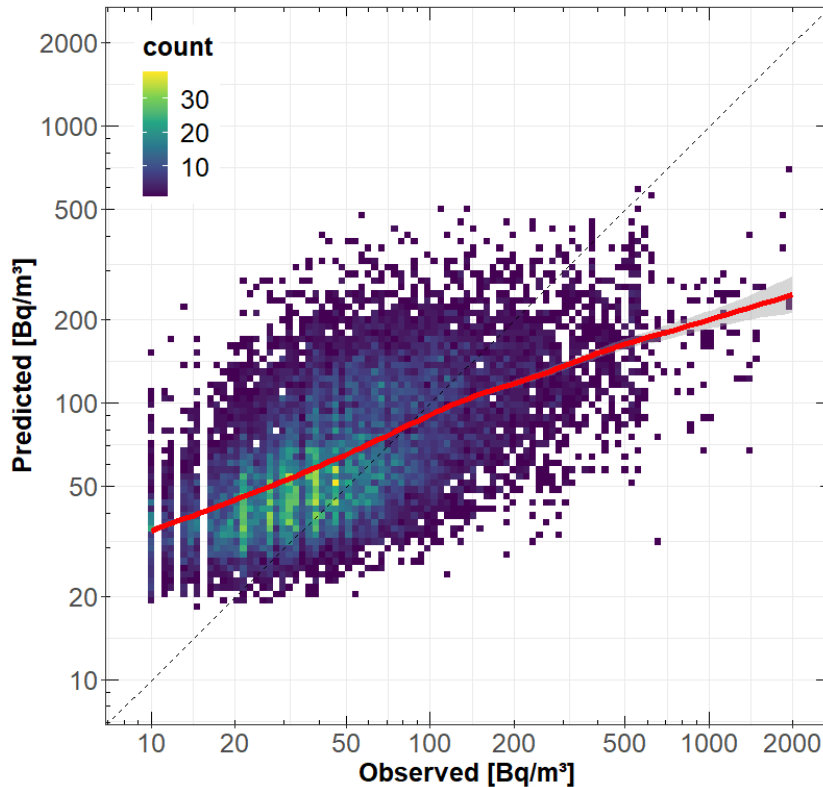


Figure 7: Model performance of quantile regression forest model for predicting the conditional mean. Please note, axes are on a log-scale. The red line shows the smoothed conditional mean estimated by a generalized additive model. Results are based on 10-fold spatial cross-validation ( $n=14,053$ ). Data is available in Supplemental Excel file; table S6.

The 80 % (10 – 90 %ile) and 50 % (25 – 75 %ile) prediction intervals cover 78.2 % and 49.1 % of test observations, respectively, which is very close to the desired values. Consequently, a good overall performance can be concluded. Moreover, the scatter of observations outside the prediction intervals is evenly distributed over the entire range of predicted values (Figure 8). Additionally, about the same proportion of the test data lies above and below the prediction interval. This observation is confirmed when focusing on specific quantiles: The quantile coverage probability (QCP) of selected quantiles is shown in Table 1 and indicates that the actual coverage is very close to the nominal coverage over the entire range of quantiles. On average, the QCP deviates from the nominal coverage by only  $\sim 1\%$ -point. Consequently, we can conclude that the prediction intervals are very accurate and reliable: the desired proportion of the data is covered by the respective intervals.

In summary, the prediction uncertainty is large but can be described accurately. Therefore, it can be assumed that propagation of the prediction uncertainty via a probabilistic procedure such as Monte Carlo sampling provides a reasonable approximation to the true variability of individual radon

concentration.

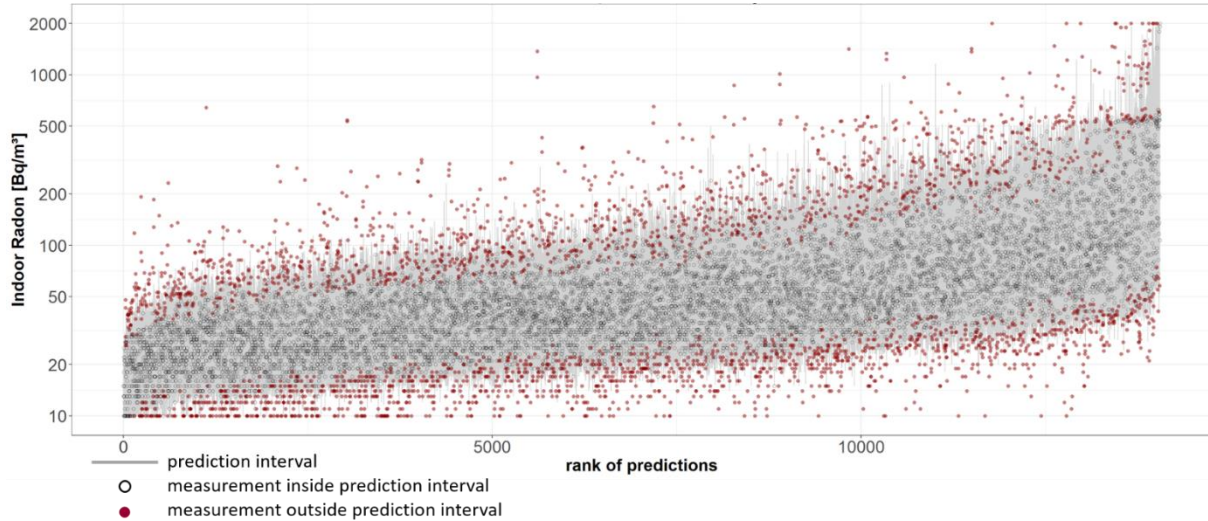


Figure 8: Prediction intervals (10-90 %ile) of quantile regression forest model vs. observed values. Predictions are shown for test data from a 10-fold spatial cross-validation. Data is sorted by increasing estimates of the conditional median. Prediction intervals are visualized as grey vertical bars. Measurements inside the prediction interval are depicted as black empty circles, predictions outside the prediction interval are depicted as dark red circles. Data is available in Supplemental Excel file; table S7.

Table 1: Quantile coverage probability of predicted quantiles.

Quantile (nominal)	Quantile coverage probability (actual)
10 %ile	11.0%
25 %ile	26.3%
50 %ile	50.9%
75 %ile	74.6%
80 %ile	79.6%
85 %ile	84.5%
90 %ile	89.0%
95 %ile	93.9%
98 %ile	96.9%

### 3.3. Indoor radon concentration

The predicted indoor radon distribution of Germany is characterized by an arithmetic mean (AM) of 63 Bq/m<sup>3</sup> (standard deviation: 147 Bq/m<sup>3</sup>) and a geometric mean of 41 Bq/m<sup>3</sup> (geometric standard deviation: 2.27). Selected quantiles of the 50 %ile, 90 %ile and 95 %ile are 36 Bq/m<sup>3</sup>, 115 Bq/m<sup>3</sup> and 180 Bq/m<sup>3</sup>, respectively. The exceedance frequencies for 100 Bq/m<sup>3</sup>, 300 Bq/m<sup>3</sup>, 600 Bq/m<sup>3</sup> and 1000 Bq/m<sup>3</sup> are 12.5 % (10.5 million people), 2.2 % (1.9 million people), 0.67 % (560.000 people) and 0.25 % (210.000 people), respectively.

Figure 9 presents the estimated quantities of indoor radon concentration at different spatial resolutions: federal states, districts and municipalities. The same data is also available on an interactive website (<https://indoor.radonmap.info>). The AM and the exceedance probability of 300 Bq/m<sup>3</sup> (>300 Bq/m<sup>3</sup>) reveal similar spatial patterns. The most affected federal states are Saxony (AM: 100 Bq/m<sup>3</sup>; probability >300 Bq/m<sup>3</sup> (P300): 5.9 %), Thuringia (AM: 103 Bq/m<sup>3</sup>; P300: 5.6 %) and Bavaria (AM: 85 Bq/m<sup>3</sup>; P300: 4.0 %). However, when focusing on the higher spatial resolution of districts or municipalities it becomes clear that affected areas also exist in Baden-Württemberg, Rhineland-Palatinate, Hesse, Northrhine-Westphalia, Saxony-Anhalt, Mecklenburg Western Pomerania, Lower Saxony and Schleswig Holstein (see top-left plot in Figure 9 for location of the federal states). At the district level, 18 districts (out of 401) exceed an AM of 150 Bq/m<sup>3</sup> as well as a 10 % probability of exceeding the 300 Bq/m<sup>3</sup> reference level. At the municipality level, about 900 municipalities (out of 10,885) exceed an AM of 150 Bq/m<sup>3</sup> as well as a 10 % probability of exceeding the 300 Bq/m<sup>3</sup> reference level. In most cases, the areas with the highest AM and P300 values are located in low mountain ranges (e.g. Erzgebirge: Saxony, Fichtelgebirge: Bavaria, Harz: Saxony-Anhalt, Lower Saxony; Black Forest: Baden-Württemberg) or the Alps (Bavaria) or in areas with moraine deposits from the recent glacial advance (Mecklenburg-Western Pomerania, Schleswig-Holstein), which have a higher geogenic radon potential.<sup>66</sup>

The quantities of AM and P300 are an indicator of the individual risk, whereas the number of people exposed to indoor radon above 300 Bq/m<sup>3</sup> (third row of Figure 9) represents an indicator of the collective risk. As a consequence of population density, the highest collective indoor radon risk can be found in big cities such as Munich, Berlin, Cologne and Hamburg even though the geogenic radon hazard is low in most of the big cities in Germany (with the exception of Munich, which has a moderate to elevated geogenic radon hazard). The contrasting spatial patterns between individual risk and collective risk confirm our previous results<sup>33,76</sup>, which had a focus on radon-exposed buildings.

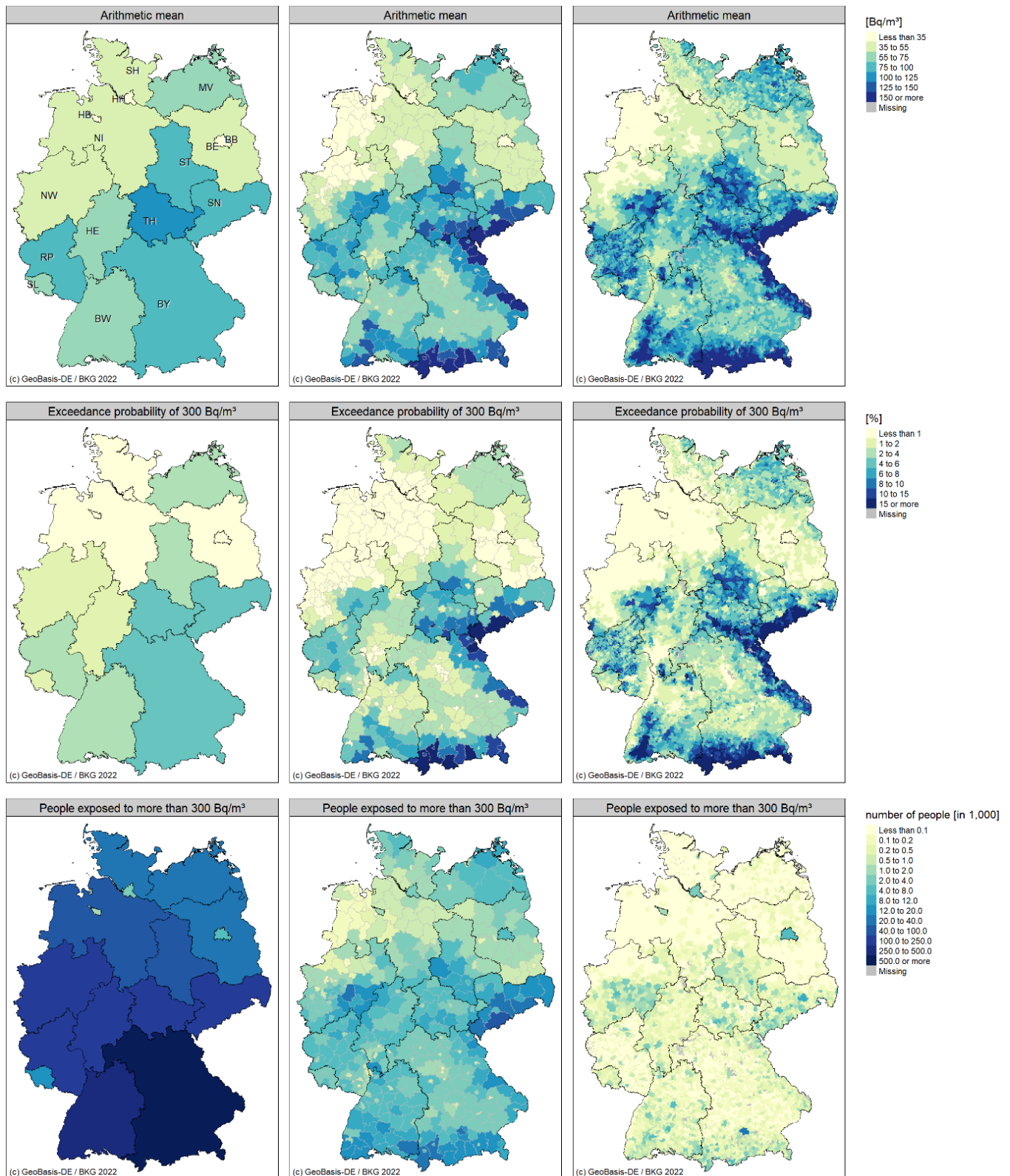


Figure 9: Maps of indoor radon characteristics, estimated with a model-based approach, at the administrative level of federal states („Bundesländer“), districts („Landkreise und kreisfreie Städte“) and municipalities („Gemeinden“) in the first, second and third column, respectively. The depicted quantities are the arithmetic mean, relative exceedance of 300 Bq/m<sup>3</sup> [%] and the number of people who are exposed to more than 300 Bq/m<sup>3</sup> in the first, second and third row. Abbreviations for federal states (see top left plot): SH – Schleswig Holstein; HH - Hamburg; MV – Mecklenburg Western Pomerania; NI – Lower Saxony; HB - Bremen; BB - Brandenburg; BE – Berlin; ST – Saxony-Anhalt; NW - Northrhine-Westphalia; SN – Saxony; TH – Thuringia; HE - Hesse; RP - Rhineland Palatinate; SL - Saarland; BY - Bavaria; BW -Baden-Württemberg. Please note, on the

*municipality level predictions are only provided for municipalities with at least 100 inhabitants (i.e., 1000 Monte Carlo samples). Interactive maps can be found at <https://indoor.radonmap.info>. Data is available in Supplemental Excel file; tables S8, S9, and S10.*

## 4. Discussion

### 4.1. Modelling approach

The sample size of the indoor radon survey was set considering the requirement to allow a robust characterization of the statistical moments at the national level. However, because of the sampling biases described above, with too many measurements in the basement and on groundfloor as well as deviations from the desired sample size in some districts (see S1 and 3.1), the measurements alone were not sufficient to provide an accurate estimate of the arithmetic mean, probability of exceeding a given concentration, etc., at the national level. In addition, the sample size was too small (intentionally; due to budget constraints) to allow characterization of indoor radon distribution at the subnational level (federal states, districts, municipalities) based on descriptive statistics alone.

The above model uses the correlation between indoor radon concentration and predictor data such as environmental conditions and building-related information. The most important predictors were identified as floor level and soil radon which is in line with many other studies where they have been identified as key factors (see 2.2 for details). Floor level describes the distance to the ground, which is usually the main source of indoor radon. Radon concentration in soil in combination with the gas permeability of the soil is the key factor for geogenic radon hazard. The other top predictors are also plausible from a physical point of view: the age of the building might reflect the quality of the buildings foundation and the building materials used, the outdoor temperature affects pressure differences between indoor and outdoor and also the tightness of isolation which in turn affects air exchange, slope determines the contact area between building and ground. The predictors precipitation (annual sum) and soil moisture (annual mean) are proxies for the local interaction of soil physical properties and climate. The related processes such as radon emanation and radon transport in the soil affect the geogenic radon potential. The wind exposure index reflects the relative terrain position (e.g., less exposed in valleys, more exposed on hilltops) which acts as a proxy for average wind speed, which can affect the indoor/outdoor pressure differences and, thus, radon entry.

The availability of point-scale building-related data and high-resolution environmental data (maximum grid cell size of 500 m) allowed characterization of indoor radon distribution even at the municipality level. Consequently, the applied modelling approach was able to: 1) correct for sampling bias, and, 2) provide predictions at the sub-national level. The analysis of model performance revealed that accurate prediction of point estimates such as the conditional mean of indoor radon is not yet possible, which is consistent with many other studies<sup>31,35,77,78</sup>. This finding is reflected in a large local prediction uncertainty and the resulting wide prediction intervals. The main reason for the large prediction uncertainty is considered to be missing relevant prediction data, which are determined by building characteristics and behaviour of the residents (air tightness of the building, ventilation intensity, heating system, etc.) as well as the possible inaccuracy of the existing predictor data (e.g. insufficient map resolution, suboptimal classification). However, as demonstrated in this study, a powerful model such as the Quantile Regression Forest (QRF), combined with currently available predictor data, allows for accurate characterization of the prediction uncertainty. QRF is increasingly applied in recent years. Many studies with varying objectives such as digital soil mapping<sup>79</sup>, heat wave prediction<sup>80</sup>, radionuclide transfer from soil to plant<sup>81</sup> or spatial prediction of groundwater levels<sup>82</sup> have proven QRFs ability to provide robust estimates of prediction intervals. The ability to provide reliable prediction intervals, in turn, allowed an effective propagation of the predictive uncertainty into indoor radon concentration variability. The latter was achieved by combining the QRF-based predictions of the conditional distributions (probability density function for each floor in each residential building) with a Monte Carlo sampling procedure. The use of high-resolution population distribution data allows population weighting of the predictions by making the sample size in the Monte Carlo sampling procedure proportional to the expected number of people per floor.

## 4.2. Uncertainty and limitations

There are several sources of uncertainty related to the applied modelling approach. Some of them can be quantified, others can only be described qualitatively. Probably the largest source of uncertainty is the lack of data on spatially resolved information on the occurrence of basements as well as on the use of basements. This information is important because in most buildings, radon concentration is greatest in basements. In this study, we parameterized basement occupancy by an "educated guess" (see 2.2.3 and S4) of 30 % basement occupancy relative to the occupancy of each upper floor for single- and two-family houses, row houses, etc., and 5 % for multi-family houses, apartment blocks, etc. A scenario analysis was performed to evaluate the impact of this decision on indoor radon concentration estimates. In this scenario analysis, the assumed values were changed to 20 % (alternative scenario 1) and 50 % (alternative scenario 2) for single- and two-family houses, townhouses etc. as well as 2 % (alternative scenario 1) and 10 % (alternative scenario 2) for multi-family houses, apartment blocks etc. The scenario analysis revealed that the choice of these parameters appeared to be more critical in rural areas because the fraction of single- and two-family houses is generally higher and thus more people live in buildings with relatively high occupation of basements. At the national level, a deviation of up to  $\pm 10$  % of the arithmetic mean can be assumed on the basis of the scenario analysis. However, this sensitivity analysis represents rather an extreme case, as it is to be expected that prevalence and occupancy rates are spatially heterogeneously distributed and therefore balance each other out to a certain extent in reality.

Model performance, such as the reliability of prediction intervals (see section 3.2.2), is evaluated at the global scale. Consequently, local deviations from the predicted concentration distribution may occur if the predictor maps are not accurate in a given area or if radon-relevant conditions exist at the local scale, that are not reflected by the predictors (e.g., in (post)-mining areas). Since the predictor maps are also the result of predictive modeling (interpolation), they are also subject to uncertainty. The more important a single predictor is, the more sensitive the final prediction becomes to the uncertainty of that predictor in that area. The most important environmental predictor (Figure 6) is soil radon concentration (see S2 for more details on mapping). In turn, an important predictor of the soil radon map is the geologic map, i.e., the classification system and spatial extent of a single geologic unit influence the soil radon map. Therefore, municipality-scale predictions should be interpreted considering the predictors used in the model (Fig. 3) and their respective values in the predictor maps (Fig. 2) at the local level, and considering possible local specifications. In general, uncertainty is expected to be significantly lower on the national scale but increases at higher spatial resolutions (see Wadoux & Heuvelink 2023<sup>83</sup> for details). In our case, uncertainty at the national scale is expected to be driven by uncertainty of basement prevalence and occupation, while uncertainty at the district or municipality scale is expected to be driven by both uncertainty of basement prevalence and occupation as well as predictor data uncertainty.

The quantification of uncertainty of spatial averages requires consideration of the spatial autocorrelation of the standardized prediction error<sup>83</sup>. However, the assumption of second-order stationarity, i.e. a constant correlation length in the entire study area, does not seem to be justified. Therefore, hybrid approaches such as regression kriging seem to be no alternative in our case. Nevertheless, the residual spatial autocorrelation does contain information about the target variable. How this information can be used optimally is a subject of current research.<sup>84-86</sup>

In general, the annual mean of indoor radon is considered to be a reliable estimate of the long-term mean value. However, several studies (see review in Antignani et al. 2021<sup>87</sup>) have shown that there are inter-annual variations at the building level. For larger areas under investigation or multiannual surveys

these year-to-year variations are likely to average out to some extent and to be of less relevance. However, since our survey was conducted in the period 2019-2021, the resulting estimates, in a strict sense, only refer to that period. The annual average of the study period could deviate from the long-term mean if there were significant large-scale changes in relevant factors such as climate (extreme years in terms of temperature or precipitation) or lifestyles that affect ventilation rates (COVID pandemic in 2020/2021), were present. Furthermore, beyond estimating the distribution of indoor radon concentrations, changing lifestyles (e.g. remote working, lockdown) also affect the occupancy of houses/apartments, which affects concentration at the individual level in terms of occupancy times.

4.3. Uncertainty at the national level can be further reduced by implementing information on the prevalence of basements and their occupancy (regionalised and differentiated by building type). Uncertainty of predictions for individual building and floors could be further reduced if spatially exhaustive data on the building material, the ventilation system and the energy efficiency status of a building (e.g. building codes, energy retrofiting) becomes available. Indoor radon distribution and radon policy

The results from the current study revealed a higher mean indoor radon concentration in Germany (AM=63 Bq/m<sup>3</sup>; section 3.3) than previously estimated by Menzler et al. (2006)<sup>88</sup>, who determined an arithmetic mean of 49 Bq/m<sup>3</sup> and a geometric mean of 37 Bq/m<sup>3</sup>. The main reason for this difference is likely to be the consideration of basement occupancy - a key factor deliberately neglected by Menzler et al. (2006) due to the lack of data at the time. The differences in the spatial patterns of indoor radon between the two studies are primarily due to 1) the availability of more and better-resolved predictor data nowadays, especially in terms of soil radon concentration and building information, and 2) the predictive modelling approach that fully reflects the distribution of radon-relevant factors in the entire population. It should be noted that possible temporal changes cannot be readily inferred from the comparison of the two studies due to methodological differences and assumptions inherent in the studies.

The presented maps of the arithmetic mean and the probability of the exceedance of the reference level of 300 Bq/m<sup>3</sup> represent the individual risk as they combine information on hazard (environmental conditions) and vulnerability (housing characteristics). The map of the total number of people exceeding the reference level, on the other hand, is a measure of collective risk. The spatial patterns are generally consistent with the maps of buildings affected by radon (i.e., expected value >300 Bq/m<sup>3</sup> on ground floor) produced by Petermann & Bossew (2021)<sup>33</sup> using a much simpler approach that built solely on geogenic radon potential as single predictor. However, noticeable differences can be observed in some areas, especially in the south and west of Germany. The number of radon-affected buildings was estimated with 350.000<sup>33</sup> which is a factor of 5 to 6 lower than the number of affected-people (above 300 Bq/m<sup>3</sup>) which was estimated with 1.9 million in this study. These figures seem plausible, since in most cases several people are affected by elevated radon concentrations if a value of over 300 Bq/m<sup>3</sup> is expected on the ground floor of a building. As a rule, however, not all persons living in this building are affected in every case, especially on the upper floors. On the other hand, people may also be affected by an exceedance of the reference value if they stay in the basement, even if the ground floor is not affected, and the building would not be classified as radon-affected.

Another interesting feature is that large cities usually have lower values (AM, P300) than the surrounding areas – and this even in cases where the city and the surrounding area have a comparable geogenic radon risk. The reason for this difference in indoor radon concentration is that the population density in urban areas is much higher than in their surrounding areas. As a result, multi-family buildings and apartment buildings are much more common in urban areas, which means that the proportion of

people living in upper floors is also greater in urban areas than in rural municipalities. In other words: In an area with the same geogenic radon hazard, indoor radon concentration would be higher in rural areas than in urban areas because more people in rural areas - due to differences in settlement patterns - live in lower floors and thus closer to the geogenic radon source.

For the sake of health protection, radon priority areas (RPAs) must be defined from 2020 onwards according to EURATOM Basic Safety Standards (EU-BSS)<sup>89</sup>, a EURATOM directive. In Germany, RPAs are delineated by the competent authorities of the federal states based on various information sources such as national radon maps or relevant local information. The formal criterion is a 10 % exceedance probability of the reference level (300 Bq/m<sup>3</sup>) in a residential building for a standard situation “ground floor of a residential building with basement” on at least 75 % of the area of the respective administrative unit. Currently, about 2 % of the area of Germany (inhabited by 1 % of the population) are designated RPAs. We found that only 9 % of the population likely to be exposed to indoor radon concentrations above 300 Bq/m<sup>3</sup> lives in RPAs. This result is consistent with our estimate of 7 % of radon-exposed buildings (i.e. expected exceedance of 300 Bq/m<sup>3</sup> on the ground floor) in a previous study<sup>76</sup>. Important to note, the exceedance probabilities presented in this study, which focus on the average concentration of the population, are not directly comparable with the reference building defined for the delineation of the RPA. However, when analysing the RPA status (yes/no) of the ten districts with the highest indoor radon concentration predictions, only four districts are fully or partially designated as RPAs - in six districts not a single municipality is a designated RPA. As far as municipalities are concerned, as shown in 3.3, in about 900 cases the exceedance probability of 300 Bq/m<sup>3</sup> (reference value) is greater than 10 % and the arithmetic mean is greater than 150 Bq/m<sup>3</sup>. However, in Germany a total of only 210 municipalities are designated as RPAs. On the one hand, the fact that only ~1 % of the population live in RPAs, but ~9 % of cases of reference value exceedances are to be expected in RPAs show the accuracy of the RPAs delineated due to the significantly higher level of affectedness. On the other hand, it becomes obvious that the vast majority of the German population (~90 %) exposed to indoor radon levels above 300 Bq/m<sup>3</sup> live outside the RPAs. We therefore recommend that these figures should be considered for policy measures in the near future to optimise radiation protection of the population.

## 5. Conclusion

A new estimate of indoor radon distribution for Germany was produced, providing information on relevant statistical characteristics such as the arithmetic mean or the exceedance probability of 300 Bq/m<sup>3</sup> at different administrative levels (country, federal state, district, municipality). Thus, updated indoor radon maps for Germany are provided.

The application of a quantile regression forest model that was trained with measurement data from a recent harmonised national indoor radon survey and high-resolution environmental and building-related predictor data provided a reliable characterisation of prediction intervals and, thus, estimation of probability density functions for each floor level of each residential building in Germany. A downstream Monte Carlo sampling procedure enabled the combination of these probability distribution functions as well as population weighting. In this way, the prediction uncertainty on the scale of individual predictions was effectively propagated into the variability at the aggregated scale of administrative units. In consequence, we were able to correct for the sampling bias (too many measurements in basements and on groundfloors) and to provide a characterization of indoor radon distribution even for municipalities where no or only a small number of measurements were available.

The results of this study could be used for epidemiological studies, e.g. for calculating the proportion of lung cancer cases attributable to radon under consideration of additional data such as smoking

behavior. Furthermore, the model could also be used in case-control studies for the prediction of indoor radon for cases for which no measured data are available.

The presented modelling approach can also be applied to other countries or regions given that a comprehensive set of indoor radon measurement data, relevant predictor data and an exhaustive data set on the residential building stock including relevant building characteristics are available.

The maps with the radon indoor predictions (<https://indoor.radonmap.info>) and the prediction model (<https://model.radonmap.info>) are available on interactive websites, which facilitates interaction with the results and increases the comprehensibility of the model.

## Acknowledgements

The indoor radon survey was funded by the German Federal Ministry for the Environment, Nature Conservation, Nuclear Safety and Consumer Protection (project 3618S12261 “Ermittlung der aktuellen Verteilung der Radonkonzentration in deutschen Wohnungen”).

Special thanks to Valentin Ziel (Federal Office for Radiation Protection, BfS) for technical support in creating the websites.

Further, we thank Felix Heinzl and Nora Fenske (both Federal Office for Radiation Protection, BfS) for discussion of the draft manuscript and valuable feedback.

We would also like to thank the Federal Agency for Cartography and Geodesy (BKG) for providing the data set on buildings and inhabitants for Germany in advance.

We are grateful to the valuable input of the editorial team and three anonymous reviewers whose critical comments contributed to the quality of this paper.

## Author contribution

Author contributions: survey design: JK, VG, PB, BH; survey realisation: JK, VG; methodology: EP, PB; data analysis: EP; modelling and software: EP; drafting the manuscript: EP; revision of original manuscript: all.

## References

1. WHO. *WHO handbook on indoor radon: a public health perspective*. 2009. 9784938987947 (Japanese) 9789241547673  
9788567870038 (Portuguese). 2009. <https://apps.who.int/iris/handle/10665/44149>
2. IARC. *IARC Working Group on the Evaluation of Carcinogenic Risks to Humans. Man-made Mineral Fibres and Radon*. IARC Monographs on the Evaluation of Carcinogenic Risks to Humans, No 43. International Agency for Research on Cancer; 1988.
3. Darby S, Hill D, Auvinen A, et al. Radon in homes and risk of lung cancer: collaborative analysis of individual data from 13 European case-control studies. *BMJ*. Jan 29 2005;330(7485):223. doi:10.1136/bmj.38308.477650.63
4. Yitshak-Sade M, Blomberg AJ, Zanobetti A, et al. County-level radon exposure and all-cause mortality risk among Medicare beneficiaries. *Environ Int*. Sep 2019;130:104865. doi:10.1016/j.envint.2019.05.059
5. Mozzoni P, Pinelli S, Corradi M, Ranzieri S, Cavallo D, Poli D. Environmental/Occupational Exposure to Radon and Non-Pulmonary Neoplasm Risk: A Review of Epidemiologic Evidence. *Int J Environ Res Public Health*. Oct 5 2021;18(19)doi:10.3390/ijerph181910466
6. Reddy A, Conde C, Peterson C, Nugent K. Residential radon exposure and cancer. *Oncol Rev*. Feb 22 2022;16(1):558. doi:10.4081/oncol.2022.558
7. Kreuzer M, Sommer M, Deffner V, et al. Lifetime excess absolute risk for lung cancer due to exposure to radon: results of the pooled uranium miners cohort study PUMA. *Radiat Environ Biophys*. Jan 3 2024;doi:10.1007/s00411-023-01049-w
8. UNSCEAR. *Sources, effects and risks of ionizing radiation*. 2020. *UNSCEAR 2019 Report, Annex B: Lung cancer from exposure to radon*.
9. Gaskin J, Coyle D, Whyte J, Krewski D. Global Estimate of Lung Cancer Mortality Attributable to Residential Radon. *Environ Health Perspect*. May 2018;126(5):057009. doi:10.1289/EHP2503
10. IARC. Cancer fact sheet. In: All cancers, editor.: The Global Cancer Observatory; 2020.
11. Commission E, Centre JR, Cinelli G, De Cort M, Tollefsen T. *European atlas of natural radiation*. Publications Office of the European Union; 2019.
12. Jelle BP. Development of a model for radon concentration in indoor air. *Science of the total environment*. 2012;416:343-350.
13. Savović S, Djordjević A, Ristić G. Numerical solution of the transport equation describing the radon transport from subsurface soil to buildings. *Radiation protection dosimetry*. 2012;150(2):213-216.
14. Demoury C, Ielsch G, Hemon D, et al. A statistical evaluation of the influence of housing characteristics and geogenic radon potential on indoor radon concentrations in France. *J Environ Radioact*. Dec 2013;126:216-25. doi:10.1016/j.jenvrad.2013.08.006
15. Cosma C, Cucos-Dinu A, Papp B, Begy R, Sainz C. Soil and building material as main sources of indoor radon in Baita-Steii radon prone area (Romania). *J Environ Radioact*. Feb 2013;116:174-9. doi:10.1016/j.jenvrad.2012.09.006
16. Casey JA, Ogburn EL, Rasmussen SG, et al. Predictors of Indoor Radon Concentrations in Pennsylvania, 1989-2013. *Environ Health Perspect*. Nov 2015;123(11):1130-7. doi:10.1289/ehp.1409014
17. Song G, Wang X, Chen D, Chen Y. Contribution of <sup>222</sup>Rn-bearing water to indoor radon and indoor air quality assessment in hot spring hotels of Guangdong, China. *Journal of Environmental Radioactivity*. 2011;102(4):400-406.
18. Chen J. A Summary of Residential Radon Surveys and the Influence of Housing Characteristics on Indoor Radon Levels in Canada. *Health Phys*. Dec 1 2021;121(6):574-580. doi:10.1097/HP.0000000000001469
19. Abbasi A, Mirekhtari F. Estimation of natural gas contribution in indoor <sup>222</sup>Rn concentration level in residential houses. *Journal of Radioanalytical and Nuclear Chemistry*. 2021;330(3):805-810. doi:10.1007/s10967-021-08024-z
20. Kummel M, Dushe C, Muller S, Gehrcke K. Outdoor (<sup>222</sup>Rn)-concentrations in Germany - part 2 - former mining areas. *J Environ Radioact*. Jun 2014;132:131-7. doi:10.1016/j.jenvrad.2014.01.011
21. Hosoda M, Nugraha ED, Akata N, et al. A unique high natural background radiation area - Dose assessment and perspectives. *Sci Total Environ*. Jan 1 2021;750:142346. doi:10.1016/j.scitotenv.2020.142346
22. Kropat G, Bochud F, Jaboyedoff M, et al. Major influencing factors of indoor radon concentrations in Switzerland. *J Environ Radioact*. Mar 2014;129:7-22. doi:10.1016/j.jenvrad.2013.11.010
23. Friedmann H. Final results of the Austrian Radon Project. *Health Phys*. Oct 2005;89(4):339-48. doi:10.1097/01.hp.0000167228.18113.27
24. Murphy P, Dowdall A, Long S, Curtin B, Fenton D. Estimating population lung cancer risk from radon using a resource efficient stratified population weighted sample survey protocol - Lessons and results from Ireland. *J Environ Radioact*. Jul 2021;233:106582. doi:10.1016/j.jenvrad.2021.106582
25. Smetsers R, Blaauboer RO, Dekkers F, Slaper H. Radon and Thoron Progeny in Dutch Dwellings. *Radiat Prot Dosimetry*. Sep 1 2018;181(1):11-14. doi:10.1093/rpd/ncy093
26. Bochicchio F, Campos-Venuti G, Piermattei S, et al. Annual average and seasonal variations of residential radon concentration for all the Italian Regions. *Radiation Measurements*. 2005;40(2-6):686-694. doi:10.1016/j.radmeas.2004.12.023

27. Tchorz-Trzeciakiewicz DE, Olszewski SR. Radiation in different types of building, human health. *Sci Total Environ*. Jun 1 2019;667:511-521. doi:10.1016/j.scitotenv.2019.02.343
28. Papaefthymiou H, Mavroudis A, Kritidis P. Indoor radon levels and influencing factors in houses of Patras, Greece. *Journal of Environmental Radioactivity*. 2003/01/01/ 2003;66(3):247-260. doi:[https://doi.org/10.1016/S0265-931X\(02\)00110-8](https://doi.org/10.1016/S0265-931X(02)00110-8)
29. Vukotic P, Antovic N, Djurovic A, et al. Radon survey in Montenegro - A base to set national radon reference and "urgent action" level. *J Environ Radioact*. Jan 2019;196:232-239. doi:10.1016/j.jenvrad.2018.02.009
30. Smetsers RCGM, Blaauboer RO, Dekkers SAJ. Ingredients for a Dutch radon action plan, based on a national survey in more than 2500 dwellings. *Journal of Environmental Radioactivity*. 2016/12/01/ 2016;165:93-102. doi:<https://doi.org/10.1016/j.jenvrad.2016.09.008>
31. Vienneau D, Boz S, Forlin L, et al. Residential radon - Comparative analysis of exposure models in Switzerland. *Environ Pollut*. Feb 15 2021;271:116356. doi:10.1016/j.envpol.2020.116356
32. Alber O, Laubichler C, Baumann S, Gruber V, Kuchling S, Schleicher C. Modeling and predicting mean indoor radon concentrations in Austria by generalized additive mixed models. *Stochastic Environmental Research and Risk Assessment*. 2023;37(9):3435-3449. doi:10.1007/s00477-023-02457-6
33. Petermann E, Bossew P. Mapping indoor radon hazard in Germany: The geogenic component. *Sci Total Environ*. Aug 1 2021;780:146601. doi:10.1016/j.scitotenv.2021.146601
34. Rezaie F, Panahi M, Bateni SM, et al. Spatial modeling of geogenic indoor radon distribution in Chungcheongnam-do, South Korea using enhanced machine learning algorithms. *Environ Int*. Jan 2023;171:107724. doi:10.1016/j.envint.2022.107724
35. Kropat G, Bochud F, Jaboyedoff M, et al. Improved predictive mapping of indoor radon concentrations using ensemble regression trees based on automatic clustering of geological units. *J Environ Radioact*. Sep 2015;147:51-62. doi:10.1016/j.jenvrad.2015.05.006
36. Nikkila A, Arvela H, Mehtonen J, et al. Predicting residential radon concentrations in Finland: Model development, validation, and application to childhood leukemia. *Scand J Work Environ Health*. May 1 2020;46(3):278-292. doi:10.5271/sjweh.3867
37. Li L, Blomberg AJ, Stern RA, et al. Predicting monthly community-level domestic radon concentrations in the greater boston area with an ensemble learning model. *Environmental Science & Technology*. 2021;55(10):7157-7166.
38. Carrion-Matta A, Lawrence J, Kang CM, et al. Predictors of indoor radon levels in the Midwest United States. *J Air Waste Manag Assoc*. Dec 2021;71(12):1515-1528. doi:10.1080/10962247.2021.1950074
39. Timkova J, Fojtikova I, Pacheroova P. Bagged neural network model for prediction of the mean indoor radon concentration in the municipalities in Czech Republic. *J Environ Radioact*. Jan 2017;166(Pt 2):398-402. doi:10.1016/j.jenvrad.2016.07.008
40. Wu P-Y, Johansson T, Sandels C, Mangold M, Mjörnell K. Indoor radon interval prediction in the Swedish building stock using machine learning. *Building and Environment*. 2023;245doi:10.1016/j.buildenv.2023.110879
41. Li L, Stern RA, Garshick E, Zilli Vieira CL, Coull B, Koutrakis P. Predicting Monthly Community-Level Radon Concentrations with Spatial Random Forest in the Northeastern and Midwestern United States. *Environmental Science & Technology*. 2023/11/21 2023;57(46):18001-18012. doi:10.1021/acs.est.2c08840
42. Appleton JD, Miles JC. A statistical evaluation of the geogenic controls on indoor radon concentrations and radon risk. *J Environ Radioact*. Oct 2010;101(10):799-803. doi:10.1016/j.jenvrad.2009.06.002
43. Hunter N, Muirhead CR, Miles JC, Appleton JD. Uncertainties in radon related to house-specific factors and proximity to geological boundaries in England. *Radiat Prot Dosimetry*. Aug 2009;136(1):17-22. doi:10.1093/rpd/ncp148
44. Bossew P, Dubois G, Tollesfen T. Investigations on indoor Radon in Austria, part 2: Geological classes as categorical external drift for spatial modelling of the Radon potential. *J Environ Radioact*. Jan 2008;99(1):81-97. doi:10.1016/j.jenvrad.2007.06.013
45. Gruber V, Baumann S, Wurm G, Ringer W, Alber O. The new Austrian indoor radon survey (ONRAP 2, 2013-2019): Design, implementation, results. *J Environ Radioact*. Jul 2021;233:106618. doi:10.1016/j.jenvrad.2021.106618
46. Barnet I, Fojtikova I. Soil gas radon, indoor radon and gamma dose rate in CZ: contribution to geostatistical methods for European atlas of natural radiations. *Radiat Prot Dosimetry*. 2008;130(1):81-4. doi:10.1093/rpd/ncn107
47. Lindsay R, Newman RT, Speelman WJ. A study of airborne radon levels in Paarl houses (South Africa) and associated source terms, using electret ion chambers and gamma-ray spectrometry. *Appl Radiat Isot*. Nov 2008;66(11):1611-4. doi:10.1016/j.apradiso.2008.01.022
48. Kemski J, Klingel R, Siehl A, Valdivia-Manchego M. From radon hazard to risk prediction-based on geological maps, soil gas and indoor measurements in Germany. *Environmental Geology*. 2008;56(7):1269-1279. doi:10.1007/s00254-008-1226-z
49. Font L, Baixeras C. The RAGENA dynamic model of radon generation, entry and accumulation indoors. *Science of The Total Environment*. 2003/05/20/ 2003;307(1):55-69. doi:[https://doi.org/10.1016/S0048-9697\(02\)00462-X](https://doi.org/10.1016/S0048-9697(02)00462-X)
50. Riley WJ, Robinson AL, Gadgil AJ, Nazaroff WW. Effects of variable wind speed and direction on radon transport from soil into buildings: model development and exploratory results. *Atmospheric Environment*. 1999/06/16/ 1999;33(14):2157-2168. doi:[https://doi.org/10.1016/S1352-2310\(98\)00374-4](https://doi.org/10.1016/S1352-2310(98)00374-4)
51. Bena E, Ciotoli G, Ruggiero L, et al. Evaluation of tectonically enhanced radon in fault zones by quantification of the radon activity index. *Sci Rep*. Dec 14 2022;12(1):21586. doi:10.1038/s41598-022-26124-y
52. Font L, Baixeras C, Moreno V, Bach J. Soil radon levels across the Amer fault. *Radiation Measurements*. 2008;43:S319-S323. doi:10.1016/j.radmeas.2008.04.072

53. Hauri DD, Huss A, Zimmermann F, Kuehni CE, Roosli M, Swiss National C. Prediction of residential radon exposure of the whole Swiss population: comparison of model-based predictions with measurement-based predictions. *Indoor Air*. Oct 2013;23(5):406-16. doi:10.1111/ina.12040
54. Gunby JA, Darby SC, Miles JC, Green BM, Cox DR. Factors affecting indoor radon concentrations in the United Kingdom. *Health Phys*. Jan 1993;64(1):2-12. doi:10.1097/00004032-199301000-00001
55. DWD - German Weather Service (DWD) - Climate Data Center. Data from: Multiannual Mean of Soil Moisture Under Grass and Sandy Loam, Period 1991–2010. 2018. *Offenbach, Germany*.
56. DWD - German Weather Service (DWD) - Climate Data Center. Data from: Multiannual Mean of Precipitation in Germany, Period 1981–2010. 2018. *Offenbach, Germany*.
57. DWD - German Weather Service (DWD) - Climate Data Center. Data from: Multiannual Mean of Air Temperature (2m) in Germany, Period 1981–2010. 2018. *Offenbach, Germany*.
58. BKG - Federal Agency for Cartography and Geodesy. Data from: Digital Elevation Model of Germany 25 m Resolution. 2018. *Frankfurt am Main, Germany*.
59. BGR. Geological Map of the Federal Republic of Germany, scale 1:250.000. Hannover, Germany: Bundesanstalt für Geowissenschaften und Rohstoffe (BGR) [Federal Institute for Geosciences and Natural Resources]; 2019.
60. BKG - Federal Agency for Cartography and Geodesy. Data from: Haushalte Einwohner Bund (HH-EW-Bund). 2022. *Frankfurt am Main, Germany*.
61. Breiman L. Random forests. *Machine learning*. 2001;45:5-32.
62. Hothorn T, Zeileis A. partykit: A modular toolkit for recursive partytioning in R. *The Journal of Machine Learning Research*. 2015;16(1):3905-3909.
63. Hothorn T, Hornik K, Zeileis A. Unbiased Recursive Partitioning: A Conditional Inference Framework. *Journal of Computational and Graphical Statistics*. 2006;15(3):651-674. doi:10.1198/106186006x133933
64. Strobl C, Boulesteix AL, Zeileis A, Hothorn T. Bias in random forest variable importance measures: illustrations, sources and a solution. *BMC Bioinformatics*. Jan 25 2007;8:25. doi:10.1186/1471-2105-8-25
65. Meinshausen N, Ridgeway G. Quantile regression forests. *Journal of machine learning research*. 2006;7(6)
66. Petermann E, Meyer H, Nussbaum M, Bossew P. Mapping the geogenic radon potential for Germany by machine learning. *Sci Total Environ*. Feb 1 2021;754:142291. doi:10.1016/j.scitotenv.2020.142291
67. CAST: 'caret' Applications for Spatial-Temporal Models. 2023. <https://github.com/HannaMeyer/CAST>, <https://hannameyer.github.io/CAST/>
68. Valavi R, Elith J, Lahoz-Monfort JJ, Guillera-Arroita G. blockCV: An r package for generating spatially or environmentally separated folds for k-fold cross-validation of species distribution models. *Methods in Ecology and Evolution*. 2019;10(2):225-232. doi:<https://doi.org/10.1111/2041-210X.13107>
69. *rriskDistributions: Fitting Distributions to Given Data or Known Quantiles*. 2017. <https://CRAN.R-project.org/package=rriskDistributions>
70. *R: A language and environment for statistical computing*. R Foundation for Statistical Computing; 2022. <https://www.R-project.org/>
71. *arrow: Integration to 'Apache' 'Arrow'*. 2023. <https://CRAN.R-project.org/package=arrow>
72. *dplyr: A Grammar of Data Manipulation*. 2023. <https://CRAN.R-project.org/package=dplyr>
73. Greenwell BM, Boehmke BC. Variable Importance Plots - An Introduction to the vip Package. *R J*. 2020;12:343.
74. Price PN, Nero AV, Gelman A. Bayesian prediction of mean indoor radon concentrations for Minnesota counties. *Health Physics*. 1996;71(6):922-936.
75. Wadoux AMJC, Heuvelink GBM, de Bruin S, Brus DJ. Spatial cross-validation is not the right way to evaluate map accuracy. *Ecological Modelling*. 2021;457doi:10.1016/j.ecolmodel.2021.109692
76. Petermann E, Bossew P, Hoffmann B. Radon hazard vs. radon risk - On the effectiveness of radon priority areas. *J Environ Radioact*. Apr 2022;244-245:106833. doi:10.1016/j.jenvrad.2022.106833
77. Ferreira A, Daraktchieva Z, Beamish D, et al. Indoor radon measurements in south west England explained by topsoil and stream sediment geochemistry, airborne gamma-ray spectroscopy and geology. *J Environ Radioact*. Jan 2018;181:152-171. doi:10.1016/j.jenvrad.2016.05.007
78. Andersen CE, Raaschou-Nielsen O, Andersen HP, et al. Prediction of 222Rn in Danish dwellings using geology and house construction information from central databases. *Radiat Prot Dosimetry*. 2007;123(1):83-94. doi:10.1093/rpd/ncl082
79. Heuvelink GBM, Angelini ME, Poggio L, et al. Machine learning in space and time for modelling soil organic carbon change. *European Journal of Soil Science*. 2021;72(4):1607-1623. doi:<https://doi.org/10.1111/ejss.12998>
80. Khan N, Shahid S, Juneng L, Ahmed K, Ismail T, Nawaz N. Prediction of heat waves in Pakistan using quantile regression forests. *Atmospheric research*. 2019;221:1-11.
81. Urso L, Petermann E, Gnädinger F, Hartmann P. Use of random forest algorithm for predictive modelling of transfer factor soil-plant for radiocaesium: A feasibility study. *Journal of Environmental Radioactivity*. 2023/12/01/ 2023;270:107309. doi:<https://doi.org/10.1016/j.jenvrad.2023.107309>
82. Koch J, Berger H, Henriksen HJ, Sonnenborg TO. Modelling of the shallow water table at high spatial resolution using random forests. *Hydrology and Earth System Sciences*. 2019;23(11):4603-4619. doi:10.5194/hess-23-4603-2019
83. Wadoux AMJC, Heuvelink GBM. Uncertainty of spatial averages and totals of natural resource maps. *Methods in Ecology and Evolution*. 2023;14(5):1320-1332. doi:10.1111/2041-210x.14106
84. Sekulić A, Kilibarda M, Heuvelink GBM, Nikolić M, Bajat B. Random Forest Spatial Interpolation. *Remote Sensing*. 2020;12(10)doi:10.3390/rs12101687
85. Hengl T, Nussbaum M, Wright MN, Heuvelink GBM, Graler B. Random forest as a generic framework for predictive modeling of spatial and spatio-temporal variables. *PeerJ*. 2018;6:e5518. doi:10.7717/peerj.5518

86. Georganos S, Grippa T, Niang Gadiaga A, et al. Geographical random forests: a spatial extension of the random forest algorithm to address spatial heterogeneity in remote sensing and population modelling. *Geocarto International*. 2019;36(2):121-136. doi:10.1080/10106049.2019.1595177
87. Antignani S, Venoso G, Ampollini M, et al. A 10-year follow-up study of yearly indoor radon measurements in homes, review of other studies and implications on lung cancer risk estimates. *Sci Total Environ*. Mar 25 2021;762:144150. doi:10.1016/j.scitotenv.2020.144150
88. Menzler S, Piller G, Gruson M, Rosario AS, Wichmann H-E, Kreienbrock L. POPULATION ATTRIBUTABLE FRACTION FOR LUNG CANCER DUE TO RESIDENTIAL RADON IN SWITZERLAND AND GERMANY. *Health Physics*. 2008;95:179-189.
89. EC. European Council. Council Directive 2013/59/Euratom of 5 December 2013 laying down basic safety standards for protection against the dangers arising from exposure to ionising radiation. Official Journal of the European Union; 2013. p. 73.

## S1. Design of indoor radon survey

The aim of the survey was to conduct a population-representative survey of indoor radon concentrations in Germany. The measurement characteristics were to be homogeneous, with standardised measurement technology and measurement duration. The survey was to consist of 12,000 measurements in 6,000 dwellings to determine the annual mean radon concentration. These criteria were set by the BfS (Federal Office for Radiation Protection), the initiator of the study.

Achieving a fully population-representative sample will not be possible because a complete list of the population for all of Germany is not available. A commercially available address register (Deutsche Post Direkt) was chosen as a practicable compromise for sampling. The address register has some limitations in terms of completeness, such as timeliness and missing addresses due to inconsistencies in data use.

The sample (participants) for Germany was selected on the basis of 401 administrative units (Kreise, Landkreise, kreisfreie Städte) to ensure that the entire area was well represented considered. The number of participants per administrative unit was calculated in proportion to the population in the unit, assuming a total number of 6,000 households.

Participants were recruited by mail. The sample was randomly selected from the address register, with no pre-filtering in terms of building style, age of the building, floor, etc. With an expected participation rate of 5%, a total of 120,000 letters were sent out. In total, however, only around 1,350 households were acquired as participants through the random mailing. Therefore, the survey was advertised via (local) media, press releases and through the BfS in order to increase the number of participants, especially in the still underrepresented administrative areas. The desired sample size was reached in this way with volunteers. A total of 8,400 households took part in the survey. Due to different response rates, the actual sample size differed from the nominal sample size in some districts (see Figure S1). Oversampling and undersampling did not follow a consistent spatial pattern (Figure S1).

Radon measurements were carried out in two habitable rooms (e.g. living room, bedroom, dining room, children's room, workroom) in each dwelling with nuclear track detectors (SSNTD) for one year according to DIN ISO 11665-4. The detectors were sent by post and returned. Participation in the measurement campaign was free of charge. The measurements were carried out between autumn 2019 and spring 2021.

In addition to the radon measurements, data on the building and the measured rooms were also collected. Information was collected on the following characteristics: type of building, year of construction, building style, number of flats in the building, number of persons in the household, presence of a basement, basement access, connection of the basement to the living area, tightness of the windows, ventilation, thermal renovation, radon remediation measures, floor, type of room, contact of the room with the ground. It was also asked whether radon measurements had already been carried out in the household, for what reason the participants took part and how they found out about the campaign (by mailing, press, etc.). Georeferencing of the building or dwelling was done via the postal address. In the end, results from 7,479 households were available. This corresponds to a response rate of around 87.5 %.

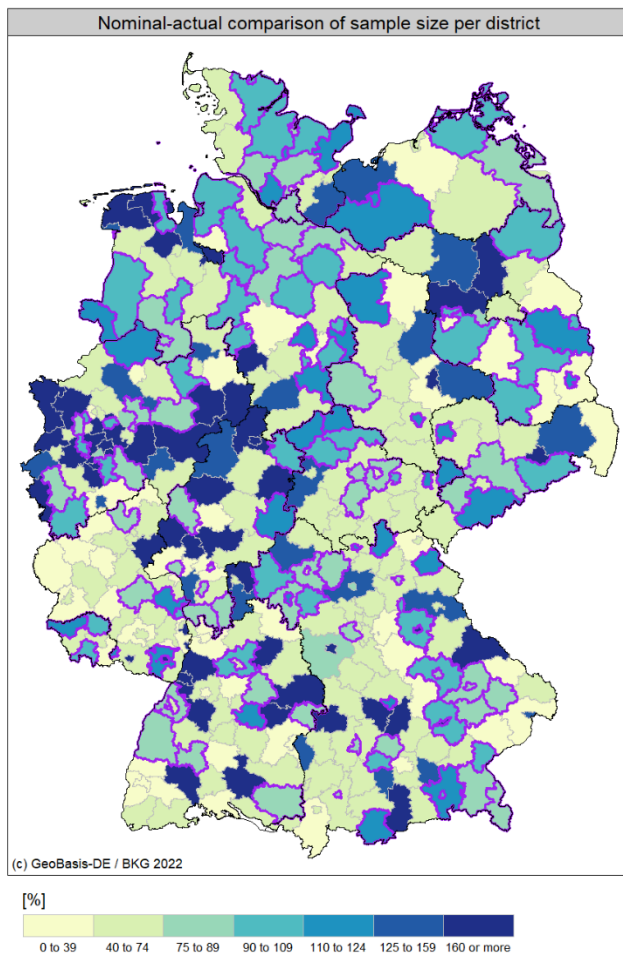


Figure S1: Spatial distribution of deviation from target sample size per district (“Landkreise und kreisfreie Städte”). Values of 100 indicate a perfect match of actual and nominal sample size, whereas values above 100 indicate oversampling and values below 100 indicate undersampling. Districts with a purple outline highlight districts with 75 % to 125 %, i.e. a deviation of maximum 25 % between actual and nominal sample size.

## S2. Environmental predictor data

In order to use optimal predictor data, German maps of soil radon concentration, soil gas permeability and outdoor radon were updated in October 2022. All available measurement data, which were available at that time, were used and state-of-the-art mapping techniques were applied. A random forest model (see 2.3 and Petermann et al. 2021<sup>1</sup> for details) was applied for mapping soil radon, soil gas permeability and outdoor radon and followed Petermann et al. (2021)<sup>1</sup>.

### Radon in soil

The available soil radon data set comprised a total of 10,184 observations of which 6768 were active short-term (soil gas sampling) and 3416 were passive long-term measurements (solid-state nuclear track detectors). The target variable was the radon activity concentration [kBq/m<sup>3</sup>] in soil in a depth of 1 m. This value was defined as the maximum of three nearby measurements (maximum distance of 5 m). Data were not transformed prior to model fitting. The RMSE was used as loss function for model fitting. Thus, due to the skewed distribution of the target variable implicitly more weight was given to high values.

The final model comprised ten predictors which were selected using a forward feature selection procedure and a 5-times repeated 10-fold spatial cross-validation approach. Selected predictors are – ranked by its importance – geology (own classification, data source BGR<sup>2</sup>), terrestrial gamma dose rate<sup>3</sup>, soil moisture<sup>4</sup>, wilting point<sup>5</sup>, a topographic wetness index (processed via SAGA algorithm<sup>6</sup>), silt fraction in topsoil<sup>7</sup>, annual precipitation<sup>8</sup>, clay fraction in topsoil<sup>7</sup>, pH of topsoil<sup>9</sup> and slope (own calculation; data source: BKG<sup>10</sup>). Geology refers to the national harmonized geological map at a scale of 1:250,000 which was re-classified with regard to radon-relevant characteristics based on lithological, chrono-stratigraphic and genetic information. Further optimization of class composition was done based on observational data in specific cases if the number of measurements was sufficiently large. Mapping of terrestrial gamma dose rate (TGDR) was done using 1079 observations of ambient dose rate (ADR). To derive TGDR contributions from cosmic rays and radionuclides in the air were subtracted from ADR.<sup>3</sup> TGDR was mapped (spatially cross-validated performance: R<sup>2</sup>=0.62, RMSE=10.5) using a random forest model utilizing a further simplified version of the aforementioned geological map and other predictors of soil, terrain and climate characteristics. The hyperparameters of the final model were optimized to *mtry*=3 and *ntree*=500. The map has a resolution of 500 m and a spatially cross-validated performance of R<sup>2</sup>=0.17, RMSE=57.4.

### Soil gas permeability

Model building for soil gas permeability was similar to the previously described one for radon soil gas mapping. A total of 9600 measurements were available. The target variable was the soil gas permeability [m<sup>2</sup>] in a depth of 1 m. This value was defined as the mean of three nearby short-term measurements (log-transformed; maximum distance of 5 m), i.e. it is the geometric mean. The final model comprised ten predictors. Selected predictors are – ranked by its importance – geology (own classification – description see above; data source BGR<sup>2</sup>), silt fraction in top soil<sup>7</sup>, mean annual outdoor air temperature<sup>11</sup>, a topographic wetness index (processed via SAGA algorithm<sup>6</sup>), sand fraction in topsoil<sup>7</sup>, slope (own calculation; data source: BKG<sup>10</sup>), potassium in topsoil<sup>9</sup>, clay fraction in topsoil<sup>7</sup> and available water capacity<sup>5</sup>.

### Outdoor radon

Model building for outdoor radon was similar to the previously described for radon soil gas and soil gas permeability. A total of 172 measurements were available. The target was the outdoor radon concentration [Bq/m<sup>3</sup>] in a height of 1.5 m above ground. Measurements were conducted in an

integrative way over a period of 3 years using solid state nuclear track detectors.<sup>12</sup> The final model comprised five predictors. Selected predictors are – ranked by its importance – distance to the Atlantic ocean defined as the shortest distance of a grid cell to the coastline of the Atlantic Ocean/North Sea (a proxy for the influence of low radon maritime air masses), local radon concentration in soil (see above), regional radon concentration in soil (arithmetic mean of 1000 nearest neighbours of radon in soil map which is roughly equivalent to the arithmetic mean within a radius of 8 km), wind exposure index (see below) and sand fraction in top soil<sup>7</sup>.

#### Wind exposure index

The wind exposure index describes the relative terrain position; it is smaller in less exposed settings (e.g., valleys) and higher in more exposed setting (e.g., mountain ridges). The index is derived from the digital elevation model in a resolution of 25 m<sup>10</sup>. It was calculated using the wind exposition algorithm<sup>13</sup> from the SAGA toolbox in QGIS.

#### Climate data: annual mean outdoor temperature, annual mean soil moisture, annual sum precipitation

Data for temperature<sup>11</sup>, precipitation<sup>8</sup> and soil moisture<sup>4</sup> refers to the reference period 1981-2010. Soil moisture refers to plant available water and is calculated for the reference soil “sandy loam under grass” with a wilting point of 13 % and field capacity of 37 %.

#### Tectonic fault density

Tectonic fault density was calculated using the geological map of Germany at a scale of 1:250,000<sup>2</sup>. This map provides line segments of tectonic boundaries. Fault density was calculated using a resolution of 100 m. Data was processed using the *pixellate* function in *spatstat*<sup>14</sup> R package.

### S3. Harmonization of building data

#### Age of building

Information on age of building for measurement data were gathered using a questionnaire (see S1). Class definition was motivated by changes in building-regulations (e.g., energy efficiency regulation) with an expected impact on air-tightness of buildings and thus a potential impact on indoor radon. Classes for age of building were defined based on the German census approach as follows: Before 1919; 1919 – 1948; 1949 – 1978; 1979 – 1986; 1987 – 1990; 1991 – 1995; 1996 – 2000; 2001 – 2004; 2005 – 2008; 2009 and later.

The building data set<sup>15</sup>, however, used a different class definition: Before 1900; 1900 – 1945; 1946 – 1960; 1961 – 1970; 1971 – 1980; 1981 – 1985; 1986 – 1995; 1996 – 2000; 2001 – 2005; 2006 – 2010; 2011 – 2015; 2016 and later. Information on age of building class definition by BKG was not available when the radon survey was launched.

Due to the misfit of class definitions, a harmonization was required to allow utilization of the predictor “age of building” for predictions of the national building stock.

Harmonized class definition of building year was as follows:

- Before 1945
- 1945 – 1980
- 1981 – 1995
- 1996 – 2005
- 2006 and later

As a consequence of class overlap the harmonization procedure was not always feasible in an unequivocal way (see table S1), i.e. some class ranges intersect which introduces ambiguity (e.g., survey class “1919 – 1948” was assigned to harmonized class “Before 1945”). However, this ambiguity considers only some classes and, in these cases, only the edges of class intervals. Therefore, reclassification of “age of building” data is expected to have only a marginal effect on the predictive performance.

*Table S1: Classification of categorical predictor “Age of building”. The harmonized class was defined as a compromise between classes provided by the survey and BKG-related classes.*

Harmonized class	Classes from survey	Classes from building data set
Before 1945	Before 1919; 1919 – 1948	Before 1900; 1900 – 1945
1945 – 1980	1949 – 1978	1946 – 1960; 1961 – 1970; 1971 – 1980
1981 – 1995	1979 – 1986; 1987 – 1990; 1991 – 1995	1981 – 1985; 1986 – 1995
1996 – 2005	1996 – 2000; 2001 – 2004	1996 – 2000; 2001 – 2005
2006 and later	2005 – 2008; 2009 and later	2006 – 2010; 2011 – 2015; 2016 and later

#### Building type

Information on building type was assigned to indoor radon observations by a spatial join between measurement locations and BKG data<sup>15</sup>. In the BKG data set buildings were classified as single- and

two-family house; townhouse/row house and semi-detached house; multi-family house; apartment building; high-rise apartment building; terrace house; farm house; office building.

### Missing data

Information on building-related characteristics in the BKG dataset was not complete for every building. Data imputation was applied in order to fill these gaps and to facilitate predictions on the full residential building stock. Missing data concerns information on “number of floor levels” (8 % missing), “building year” (1 % missing) and “building type” (1 % missing).

Missing data on building type was imputed by using information on the number of households. If number of households was  $\leq 2$ , then building type “Single- and two-family house” was imputed. If number of households was  $> 2$ , then building type “Multi-family house” was imputed.

Missing data on number of floor levels was imputed by using information on building type, age of building and number of households. If data on building type, age of building and number of households was available, a linear model (R package *stats*, function *lm*<sup>16</sup>) using the aforementioned information as predictors and number of floor levels as target was built with all data from the same chunk (see 2.3.6), i.e. a local model was built. The rounded predicted value of floor level was used for imputation. In a few cases, no data on building type and age of building was available. In these cases, the number of floor levels was estimated using a linear model with the number of households as single predictor and the rounded predicted value was used for imputation.

Missing data for age of building was not imputed because in the survey data a class with “NA” values for age of building exists to which these cases were assigned.

#### S4. Parameterization of basement occupation

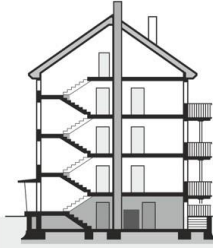
Example 1: single-family house, 2 floors, 2 inhabitants				Example 2: apartment house, 4 floors, 25 inhabitants			
	Factor	Inh./floor	n		Factor	Inh./floor	n
	1	0.87	9		1	4.95	50
	1	0.87	9		1	4.95	50
	0.3	0.26	3		1	4.95	50
					1	4.95	50
					0.05	0.25	3

Figure S2: Parameterization of basement occupation.

In case of single- and two-family houses and townhouses the basement occupation was assumed to be 30 % relative to upper floor occupation (factor 0.3). For all other building types (multi-family house; apartment building; high-rise apartment building; terrace house; farm house; office building) basement occupation was assumed to be 5 % relative to upper floor occupation (factor 0.05)

## S5 Model interpretation: partial dependence plots

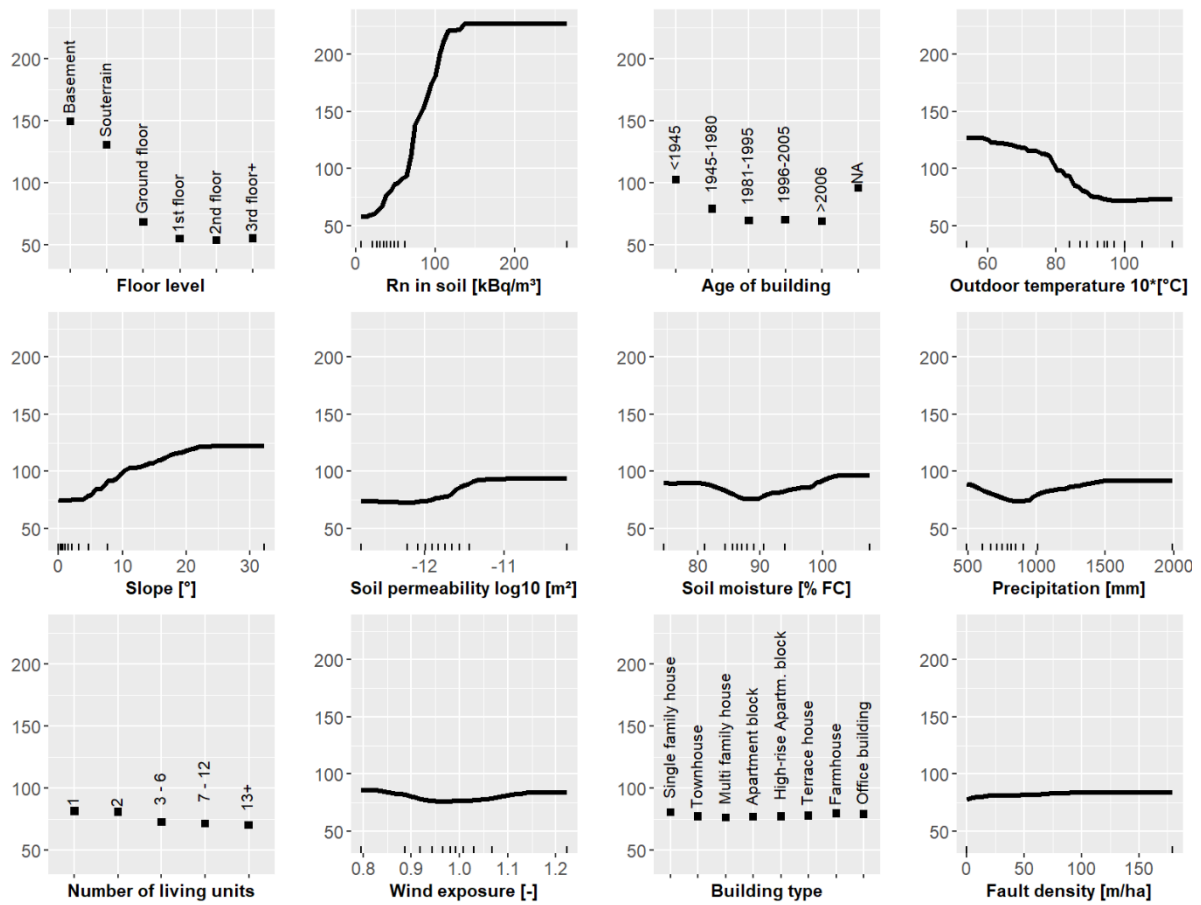


Figure S3: Partial dependence plots of quantile regression forest model for predicting indoor radon concentration. The vertical axis shows the predicted values of the indoor radon concentration [ $Bq/m^3$ ]. The small vertical bars on the x axis indicate minimum, maximum and deciles of the predictor value range for numeric predictors. The labels in the plot refer to the levels of categorical predictors.

## References

1. Petermann E, Meyer H, Nussbaum M, Bossew P. Mapping the geogenic radon potential for Germany by machine learning. *Sci Total Environ*. Feb 1 2021;754:142291. doi:10.1016/j.scitotenv.2020.142291
2. BGR. Geological Map of the Federal Republic of Germany, scale 1:250.000. Hannover, Germany: Bundesanstalt für Geowissenschaften und Rohstoffe (BGR) [Federal Institute for Geosciences and Natural Resources]; 2019.
3. Bossew P, Cinelli G, Hernandez-Ceballos M, et al. Estimating the terrestrial gamma dose rate by decomposition of the ambient dose equivalent rate. *J Environ Radioact*. Jan 2017;166(Pt 2):296-308. doi:10.1016/j.jenvrad.2016.02.013
4. DWD - German Weather Service (DWD) - Climate Data Center. Data from: Multiannual Mean of Soil Moisture Under Grass and Sandy Loam, Period 1991–2010. 2018. *Offenbach, Germany*.
5. Tóth B, Weynants M, Pásztor L, Hengl T. 3D soil hydraulic database of Europe at 250 m resolution. *Hydrological Processes*. 2017;31(14):2662-2666. doi:10.1002/hyp.11203
6. Böhner J, Selige T. Spatial prediction of soil attributes using terrain analysis and climate regionalization. *Gottinger Geographische Abhandlungen*. 01/01 2002;115
7. Ballabio C, Panagos P, Monatanarella L. Mapping topsoil physical properties at European scale using the LUCAS database. *Geoderma*. 2016;261:110-123. doi:10.1016/j.geoderma.2015.07.006
8. DWD - German Weather Service (DWD) - Climate Data Center. Data from: Multiannual Mean of Precipitation in Germany, Period 1981–2010. 2018. *Offenbach, Germany*.
9. Ballabio C, Lugato E, Fernandez-Ugalde O, et al. Mapping LUCAS topsoil chemical properties at European scale using Gaussian process regression. *Geoderma*. Dec 1 2019;355:113912. doi:10.1016/j.geoderma.2019.113912
10. BKG - Federal Agency for Cartography and Geodesy. Data from: Digital Elevation Model of Germany 25 m Resolution. 2018. *Frankfurt am Main, Germany*.
11. DWD - German Weather Service (DWD) - Climate Data Center. Data from: Multiannual Mean of Air Temperature (2m) in Germany, Period 1981–2010. 2018. *Offenbach, Germany*.
12. Kummel M, Dushe C, Muller S, Gehrcke K. Outdoor (222)Rn-concentrations in Germany - part 1 - natural background. *J Environ Radioact*. Jun 2014;132:123-30. doi:10.1016/j.jenvrad.2014.01.012
13. Böhner J, AntoniĆ O. Chapter 8 Land-Surface Parameters Specific to Topo-Climatology. In: Hengl T, Reuter HI, eds. *Developments in Soil Science*. Elsevier; 2009:195-226.
14. *Spatial Point Patterns: Methodology and Applications with R*. Chapman and Hall/CRC Press; 2015. <https://www.routledge.com/Spatial-Point-Patterns-Methodology-and-Applications-with-R/Baddeley-Rubak-Turner/p/book/9781482210200/>
15. BKG - Federal Agency for Cartography and Geodesy. Data from: Haushalte Einwohner Bund (HH-EW-Bund). 2022. *Frankfurt am Main, Germany*.
16. *R: A language and environment for statistical computing*. R Foundation for Statistical Computing; 2022. <https://www.R-project.org/>
17. *rriskDistributions: Fitting Distributions to Given Data or Known Quantiles*. 2017. <https://CRAN.R-project.org/package=rriskDistributions>
18. *arrow: Integration to 'Apache' 'Arrow'*. 2023. <https://CRAN.R-project.org/package=arrow>
19. *dplyr: A Grammar of Data Manipulation*. 2023. <https://CRAN.R-project.org/package=dplyr>